Click Here for Full Article

Large-scale deformation in a locked collisional boundary: Interplay between subsidence and uplift, intraplate stress, and inherited lithospheric structure in the late stage of the SE Carpathians evolution

L. Matenco,[1] G. Bertotti,[1] K. Leever,[1] S. Cloetingh,[1] S. M. Schmid,[2] M. Tărăpoancă,[3] and C. Dinu[4]

Received 29 January 2006; revised 12 March 2007; accepted 30 March 2007; published 4 August 2007.

[1] The interplay between slab dynamics and intraplate stresses in postcollisional times creates large near-surface deformation, particularly in highly bent orogens with significant lateral variations in mechanical properties. This deformation is expressed through abnormal foredeep geometries and contrasting patterns of vertical movements. Intraplate folding is often the controlling mechanism, particularly when the orogenic belt is locked. The study of these tectonic processes in the SE Carpathians indicates a generalized subsidence period during latest Miocene–Pliocene times driven by the slab-pull and an intraplate folding due to an overall Quaternary inversion. The latter accommodates ~5 km ESE-ward movement of this area with respect to the neighboring units, which creates complicated three-dimensional deformation patterns potentially driven at a larger scale by the interaction between the Adriatic indentor and the entire Carpathians system. The lithospheric anisotropy inherited from the subduction times concentrates strain and induces large-scale deformation far away from the active plate margins. This anisotropy is dynamic because of deep mantle processes related to the subducted slab during postcollisional times, such as thermal reequilibration or increase in slab dip. **Citation:** Matenco, L., G. Bertotti, K. Leever, S. Cloetingh, S. M. Schmid, M. Tărăpoancă, and C. Dinu (2007), Large-scale deformation in a locked collisional boundary: Interplay between subsidence and uplift, intraplate stress, and inherited lithospheric structure in the late stage of the SE Carpathians evolution, *Tectonics*, *26*, TC4011, doi:10.1029/2006TC001951.

[1]Netherlands Centre for Integrated Solid Earth Sciences, Faculty of Earth and Life Sciences, Vrije Universiteit, Amsterdam, Netherlands.
[2]Geologisch-Paläontologisches Institut, University of Basel, Basel, Switzerland.
[3]Rompetrol SA, Exploration&Production, Bucharest, Romania.
[4]Faculty of Geology and Geophysics, University of Bucharest, Bucharest, Romania.

Copyright 2007 by the American Geophysical Union.
0278-7407/07/2006TC001951$12.00

1. Introduction

[2] The evolution of foredeep basins adjacent to orogenic chains is commonly explained in terms of flexure due to thrust loading which generally forms wedge-shaped foreland basins [e.g., *Beaumont*, 1981; *Batt and Braun*, 1999]. During the main collisional phase, when nonthinned lithosphere of the lower plate arrives at the subduction zone, the system overthickens and subduction halts. Processes that postdate this collision are related to isostatic compensation and erosional unloading, possibly controlled by climatic changes [e.g., *Garcia-Castellanos*, 2002].

[3] This standard orogenic evolution is often not compatible with geological observations, which indicate excessive differential vertical movements in the foredeep during the postcollisional stage [e.g., *Bertotti et al.*, 2001]. Significant deformation can result from effects inherited from processes acting during the oceanic subduction stage, such as slab detachment [e.g., *Wortel and Spakman*, 2000], delamination [e.g., *Sacks and Secor*, 1990] or thermal reequilibration [*Toussaint et al.*, 2004]. During postcollisional times, these mantle processes compete with intraplate type of mechanisms, such as changes in the regional stress regime [e.g., *Horváth*, 1993] due to far-field stresses [e.g., *Ziegler et al.*, 1995] and result in deformation such as crustal and/or lithospheric folding [e.g., *Cloetingh et al.*, 1999]. The discrimination between these two types of processes should be rather straightforward through the quantification of vertical movements in the orogen and its foreland [e.g., *Bertotti et al.*, 2003].

[4] The Carpathians represent an optimal site for studying these postcollisional processes linked to the development of "unusual" foredeeps [e.g., *Matenco et al.*, 2003]: Significant differential vertical motions occurred along the orogen [*Sanders et al.*, 1999], as well as lateral variations in continental collision mode [*Cloetingh et al.*, 2004]. One can also study Quaternary topography (Figure 1a) in areas underlain by high-velocity upper mantle bodies such as the seismically active Vrancea region [e.g., *Radulian et al.*, 2000; *Weidle et al.*, 2005], exhibiting the largest present-day strain concentration in continental Europe [*Wenzel et al.*, 1999].

[5] At shallow crustal levels, much attention has recently been given to the kinematics of orogenic thrusting [e.g., *Matenco and Bertotti*, 2000, and references therein] and variations in mountain chain uplift [e.g., *Sanders et al.*,

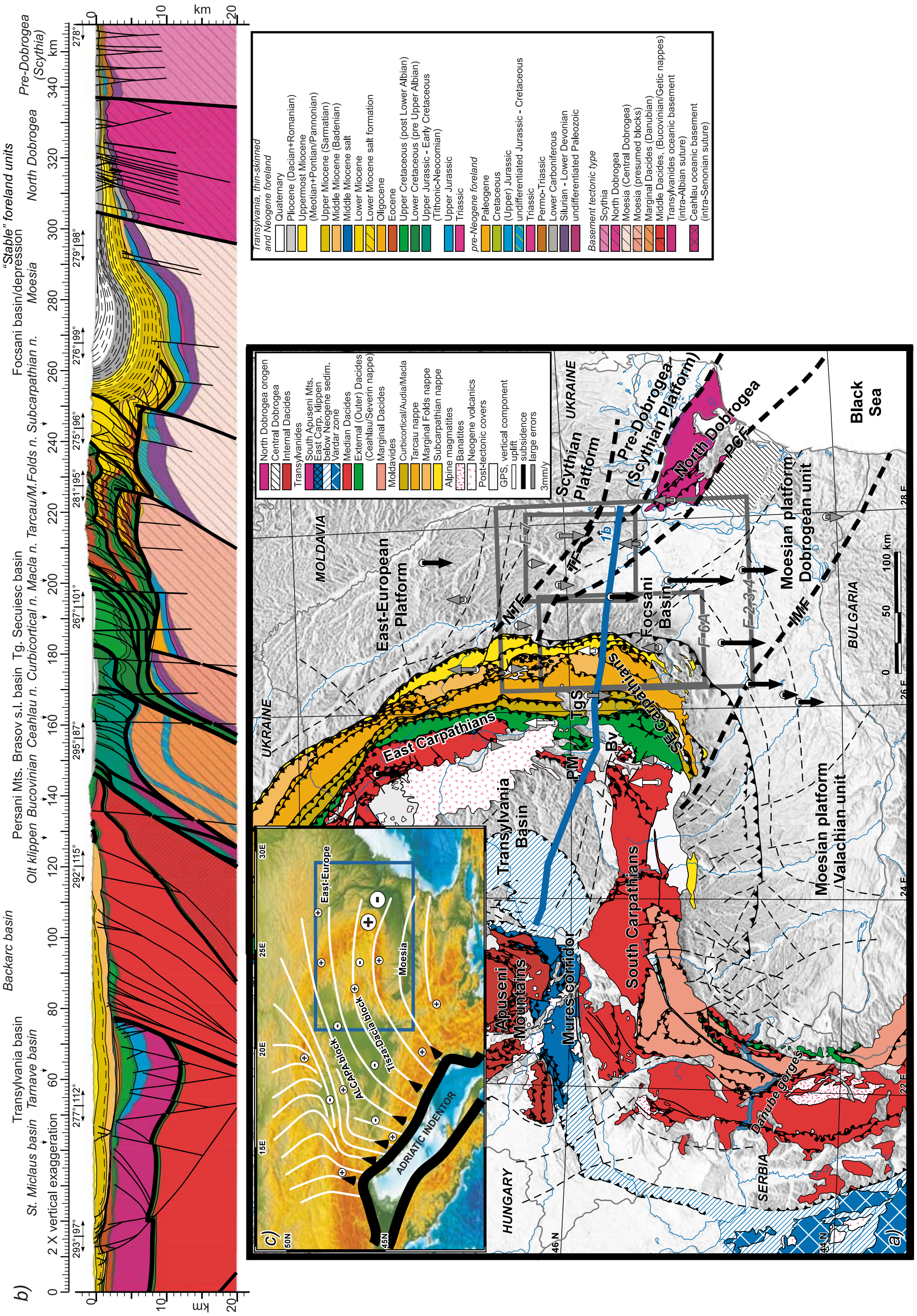

Figure 1

1999] in relationship with the flexure of a foreland [e.g., *Zoetemeijer et al.*, 1999] with an unusual foredeep basin [e.g., *Tărăpoancă et al.*, 2003] (Figure 1b). These lateral variations directly reflect different mechanics and geometries of the subducting plate [e.g., *Cloetingh et al.*, 2004]. At the deep lithospheric level, the Carpathians represent a type area for popular models such as slab retreat [e.g., *Royden*, 1993], various types of slab detachment [e.g., *Wortel and Spakman*, 2000; *Weidle et al.*, 2005, and references therein] or slab delamination [e.g., *Gvirtzman*, 2002; *Knapp et al.*, 2005].

[6] Recent studies have proven that major orogenic deformation in the mountain chain is coeval with subsidence in the lower plate, reflecting late Miocene collision in all sectors of the Carpathians [e.g., *Matenco et al.*, 2003; *Bertotti et al.*, 2003]. The mechanical and geometrical contrast between the East European/Scythian and Moesian blocks (Figures 1a and 1c) had the highest impact onto these last stages of Miocene shortening which predate the Focşani foredeep subsidence (Figure 1b). Its deformation features are not directly related to orogenic shortening mechanisms as previously inferred but to deep-seated variations in the mechanics of collision [*Cloetingh et al.*, 2004].

[7] A spectacular feature is the genesis and evolution of the Focşani depression (Figure 1b), an up to 13 km deep Neogene basin [*Tărăpoancă et al.*, 2003] restricted to a narrow area of the SE Carpathians (Figure 1a). A thick postorogenic fill was deposited on top of the late Miocene syncollisional sediments (Figures 1b and 2) [see also *Lăzărescu et al.*, 1983], strata steeply dipping away toward the foreland at the western flank of this basin, which is in apparent contradiction with the standard foredeep geometry. Unusual high topography is observed along this western flank, i.e., far out of the orogenic nappe system (Figure 3). These findings suggest that the foreland of the SE Carpathians was subjected to tectonic deformation after the main late Miocene collisional event, controlled by the inherited, preexisting structures of both upper and lower plates.

[8] The main purpose of this paper is to integrate field studies on the kinematics of deformation with basin studies to constrain the geometry and mechanisms of latest Miocene to Quaternary (active) tectonics in the SE Carpathians Bend Zone. We document the structural effects through field mapping of potentially active structures, correlated with analysis of industrial seismic lines and geomorphological patterns.

2. Evolution of the Foreland of the SE Carpathians

[9] The Romanian Carpathians represent an arcuate belt formed in response to the Triassic to Tertiary evolution of three continental blocks. The first two are referred to as Internal and Median Dacides, respectively [*Săndulescu*, 1980, 1988], also referred to as Tisza and Dacia blocks [*Balla*, 1986; *Csontos and Vörös*, 2004] and found to the west and south. The third one is formed by the East European, Scythian and Moesian platforms found to the east and north [*Săndulescu*, 1984; *Săndulescu and Visarion*, 1988; *Visarion et al.*, 1988b] (Figures 1a and 1c). These blocks were formerly separated by two oceanic domains,

Figure 1. (a) Tectonic map of the Romanian Carpathians overlying a shaded relief map [after *Săndulescu*, 1984; *Visarion et al.*, 1988b; *Matenco et al.*, 2003]. Topography is taken from the Shuttle Radar Topography Mission (SRTM) database [*Rabus et al.*, 2003]. Arrows represent GPS vertical measurements plotted after *van der Hoeven et al.* [2005], and dashed lines are faults buried below posttectonic covers. Note the location of the two Alpine suture zones in the intra-Carpathians units, i.e., the Transylvanides in the South Apuseni Mountains and below the Neogene sediments of Transylvania back-arc basin [cf. *Dewey*, 1980] and the more external Ceahlău/Severin nappe/ocean. Note also the abnormal topographic elevations in the Moesian domain outside of the main thrust front, i.e., in the foreland of the orogen near the Focşani basin. The Dacic basin is juxtaposed over the Moesian platform and the prolongation of North Dobrogea orogen, the later two units being buried below the foredeep sediments. Gray rectangles mark the location of Figures 2, 3, 4, 6a, and 7. Bv, Braşov basin; IMF, Intramoesian fault; NTF, New Trotus Fault; PCF, Peceneaga-Camena fault; PM, Persani Mountains; TF, Trotus fault; TgS, Tîrgu. Secuiesc basin; description in the text. Projection Romanian Stereo70. (b) Regional-scale section across the Romanian Carpathians displaying the relationship between the hinterland units (including the Neogene Transylvania basin), the contact zone between upper and lower plates (Persani Mountains–Braşov Basin), the external thin-skinned nappe pile and the foredeep. The location of the cross section is given in Figure 1a. The structure of the Transylvania basin, external nappes, and the foreland is after *Matenco and Bertotti* [2000] and according to the results of this study and the deep structure below the Braşov basin and pre-Neogene sequence of the lower plate [after *Ştefănescu et al.*, 1988]. Note that the basal sole thrust of the Carpathian flysch nappes has been subsequently folded and truncated by high-angle reverse faults. The entire "undeformed" foredeep sequence is folded up to subvertical positions during postnappe emplacement times. The suture zone of Late Cretaceous subduction and closure of the Ceahlău/Severin ocean is located between middle Dacides and Marginal Dacides, the presumed Danubian block representing a distal part of Moesia [see also *Visarion et al.*, 1988b]. (c) Topography of the Carpathians-Dinarides-Pannonian system in central Europe. White lines are the distribution of present-day maximum horizontal stress [after *Bada et al.*, 2001]. Positive and negative signs mark roughly the areas under Quaternary uplift and subsidence. Larger symbols in the SE Carpathians illustrate the one magnitude higher vertical movements than elsewhere. Thick black line marks the position of the Adriatic microplate, and the black arrows mark its inferred direction of movement [see also *Pinter et al.*, 2005]. Blue box represents the location of Figure 1b. For further description, see text. Projection latitude/longitude (WGS84). M, marginal; s.l., senso largo; n, nappe.

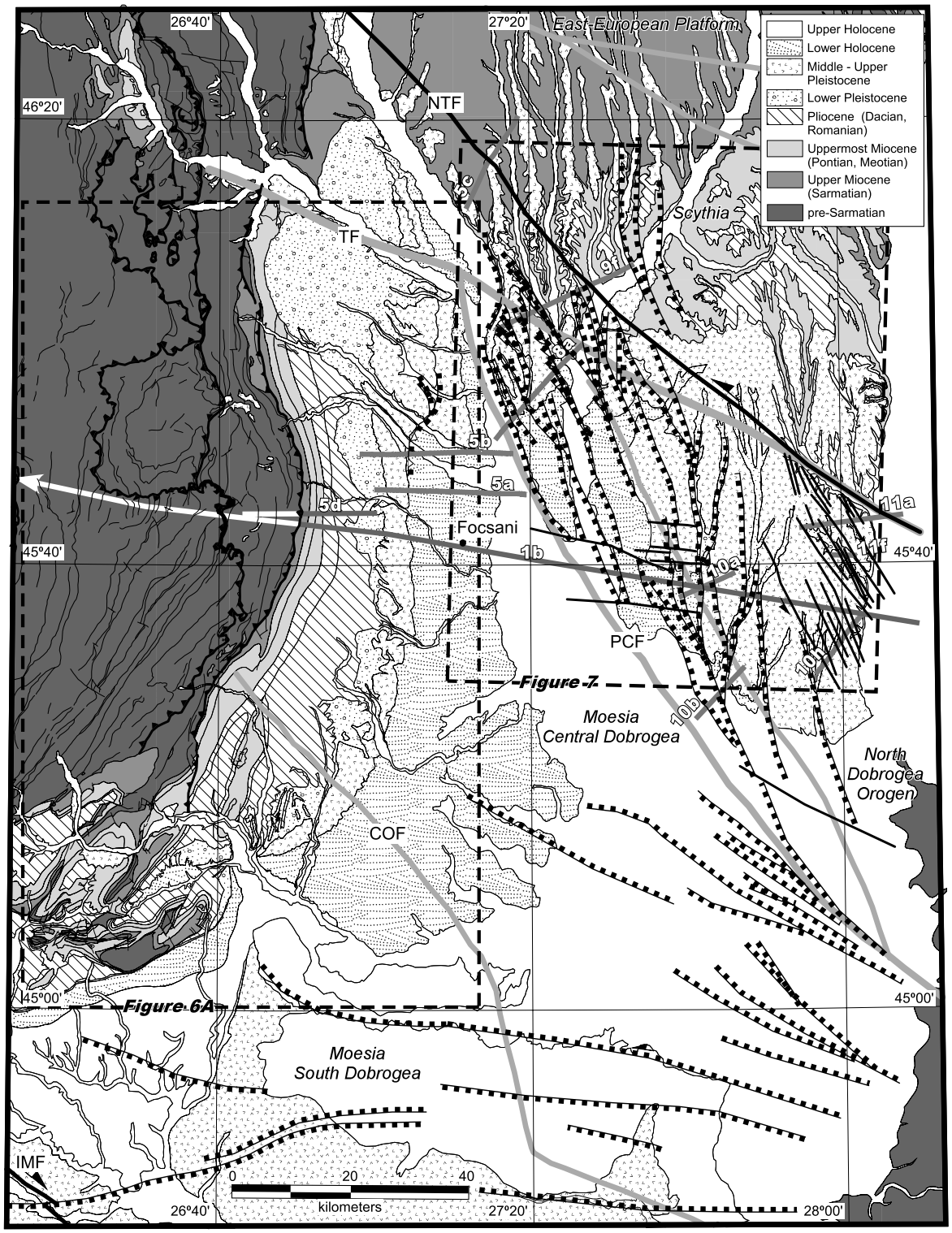
26°40'
27°20'
East-European Platform
46°20'
NTF
TF
Scythia
Upper Holocene
Lower Holocene
Middle - Upper Pleistocene
Lower Pleistocene
Pliocene (Dacian, Romanian)
Uppermost Miocene (Pontian, Meotian)
Upper Miocene (Sarmatian)
pre-Sarmatian
5b
5a
5d
Focsani
1b
45°40'
11a
10a
PCF
10b
Figure 7
Moesia
Central Dobrogea
North
Dobrogea
Orogen
COF
45°00'
Figure 6A
Moesia
South Dobrogea
IMF
0
20
40
kilometers
26°40'
27°20'
28°00'

Figure 2

whose remainders are found in the Transylvanides (Mureş-Internal Vardar zone) to the west and south, and the Outer Dacidian trough (Ceahlău/Severin ocean) to the east and north [*Săndulescu*, 1984] (Figures 1a and 1b). The Transylvanides ocean initially opened in Triassic times, evolved as a passive margin during the Early Cretaceous and was finally closed during continental collision in the Albian [e.g., *Săndulescu and Visarion*, 1977]. The more external partly oceanic basin of the Outer Dacidian basin formed in the Late Jurassic and evolved in a passive margin setting in respect to the Median Dacides throughout the Early Cretaceous. The only sedimentary cover of this domain still preserved and known to have been deposited over an oceanic basement is of Upper Jurassic–Lower Cretaceous age is preserved in the Ceahlău/Severin nappe (Figure 1), which was successively thrusted during the intra-Albian and intra-Senonian tectonic events [e.g., *Ştefănescu et al.*, 1988]. As a result, the slab of the Outer Carpathians is ~160–105 Ma old and has been completely subducted at ~75 Ma. The younger sediments of this basin still preserved in the outer flysch belt (Moldavides) were exclusively deposited over the eastern passive continental margin in respect to the Outer Dacides. These younger sediments were detached from their original basement by thin-skinned thrusting and transpression during the much later Miocene orogeny [see also *Săndulescu*, 1988; *Visarion et al.*, 1988b]. Shortening was interrupted by periods of orogen-parallel extension during the Paleogene–early Miocene [e.g., *Schmid et al.*, 1998; *Răbăgia and Matenco*, 1999; *Matenco and Schmid*, 1999].

2.1. Overall Kinematics of Orogeny

[10] The East Carpathians are made up by a stack of basement (Bucovinian) nappes with crystalline rocks and a Mesozoic sedimentary cover (Median Dacides), tectonically overlying a thin-skinned nappe system, i.e., the Ceahlău nappe (Outer Dacides), Convolute Flysch, Audia/Macla, Tarcau and Marginal Folds nappes (internal Moldavides) (Figure 1). The latter are thrust over the Subcarpathian nappe (external Moldavides). Thrusting took place in a foreland propagating sequence, nappes being deformed successively from hinterland (latest Cretaceous in case of the Outer Dacides) to foreland (Miocene in case of the Moldavides). Miocene thrusting culminated in the Sarmatian, ending in the Late Sarmatian (early late Miocene, 11 Ma), when the Subcarpathian nappe was thrust on top of the sedimentary cover of the undeformed foreland (European, Scythian and Moesian platforms) [*Săndulescu*, 1988, *Visarion et al.*, 1988a, 1988b] (Figure 1a). The geometry and kinematics of thrusting changed along strike as a consequence of the preexisting structural grain and thicknesses of sedimentary packages [e.g., *Ellouz and Roca*, 1994; *Matenco and Bertotti*, 2000]. Total shortening across the Moldavides amounts to ~160 km [*Roure et al.*, 1993; *Ellouz et al.*, 1994].

[11] During the Pliocene-Quaternary, a separate and later out-of-sequence contractional event was recorded at the junction between East and South Carpathians, i.e., the ''Wallachian'' phase [*Săndulescu*, 1988]. This led to WSW–ENE striking high-angle reverse faults that affected all the previously stacked tectonic units in the SE-most Carpathian corner (Figure 2) and folding of the latest Miocene–Pliocene postcollisional cover [e.g., *Morley*, 1996; *Hippolyte and Săndulescu*, 1996]. All structures formed during the Miocene and Pliocene-Qaternary deformation events were distorted by widespread salt diapirism nucleating near or along thrust planes [*Ştefănescu et al.*, 2000].

2.2. Inherited Structure and Geometry of the Foreland Units

[12] The undeformed foreland of the Romanian Carpathians is composed of two relatively stable areas, the East European-Scythian and Moesian platforms, partly separated by the North Dobrogea orogen [*Visarion et al.*, 1988a, 1988b] (Figure 1a).

[13] The East European/Scythian platform is bounded to the south by the Trotus fault (Figures 1 and 2). It represents a cold Precambrian block [*Săndulescu and Visarion*, 1988] with an old thermotectonic age (>150 Ma), exhibiting a 40–45 km thick crust [*Rădulescu*, 1988] and is overlain by 3–6 km thick middle-upper Miocene (Badenian-Sarmatian) sediments, with a typical foredeep-wedge geometry [*Dicea*, 1995].

[14] The Moesian platform is found south and west of the Trotus and Peceneaga-Camena faults, respectively, and represents a Precambrian block incorporated in the Epihercynian European platforms [*Săndulescu*, 1984]. It is composed of two parts, separated by the crustal-scale Intramoesian Fault [*Visarion et al.*, 1988b] (Figures 1b and 2). In the sector adjacent to the SE Carpathians (Dobrogean block), the Moesian platform is characterized by a 38–40 km thick crust [*Diehl et al.*, 2005], with significant thinning below the Neogene sediments of the

Figure 2. Geological map of the postcollisional (post-middle Sarmatian/late Miocene) main stratigraphic units in the central southern part of the East Carpathians foreland (stratigraphic units modified after 1:200,000 maps published by the Geological Institute of Romania) with the location of the active fault system depicted by the present study, location in Figure 1. Light gray lines represent major pre-Neogene tectonic lineaments [after *Visarion et al.*, 1988b]. COF, Capidava-Ovidiu fault. For other fault abbreviations, see Figure 1. Dark gray lines represent the location of interpreted seismic lines in Figures 5, 8, 9, 10, and 11. All faults drawn in the foreland are controlled by seismic lines. Sediments ages become younger from west, east, and north toward the Focşani basin depocenter (Figure 4a). Thick lines in the orogenic nappes are faults formed during shortening and collision (middle-late Miocene). Thick lines in the foreland are faults formed during Quaternary times. These are all documented either through seismic studies or surface observations. However, only a limited number of these were exemplified in the present study. For other figure conventions and location, see Figure 1.

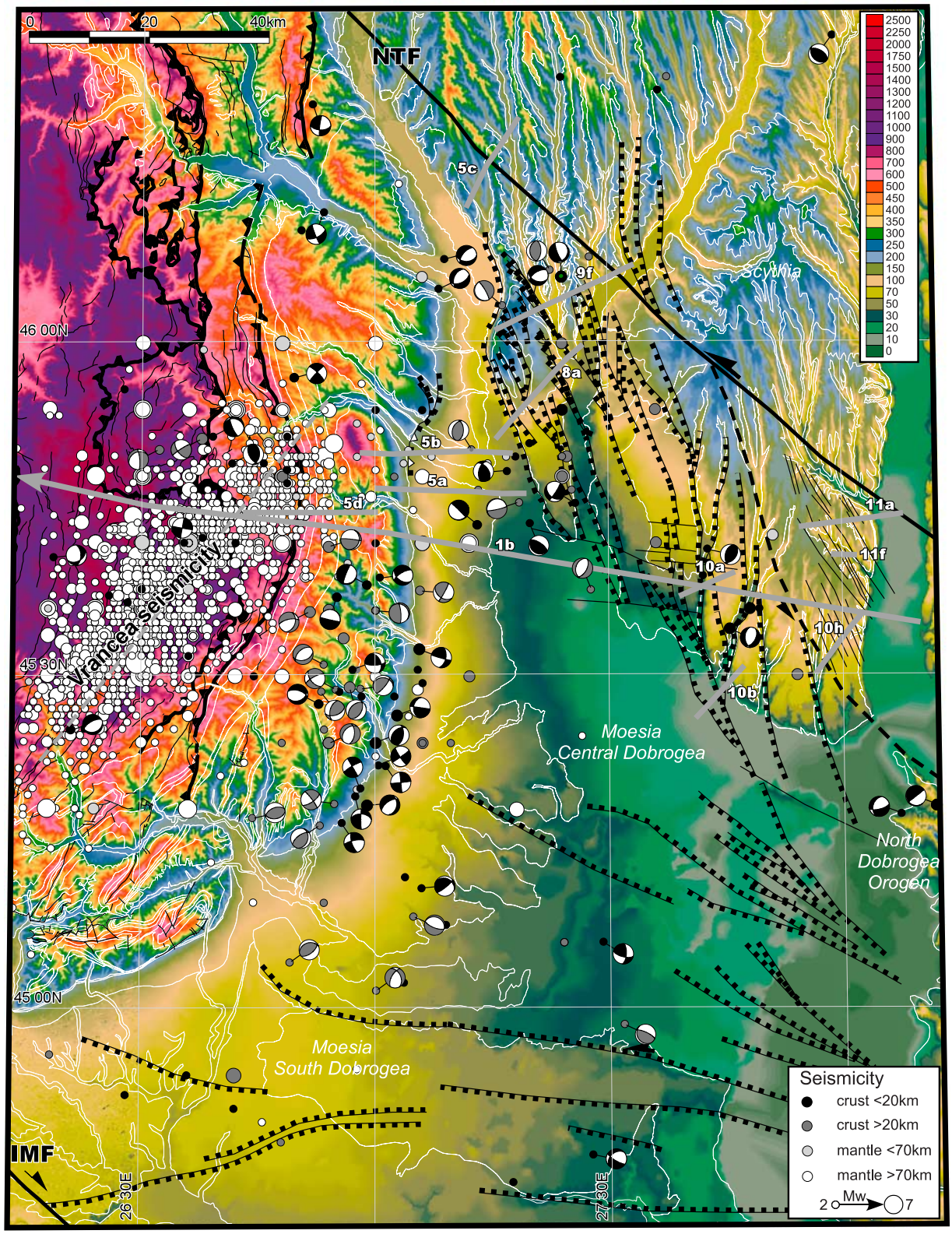
0
20
40km
NTF
5c
9f
Scythia
46 00N
8a
5b
5a
5d
11a
1b
11f
10a
Vrancea seismicity
10h
45 30N
10b
Moesia
Central Dobrogea
North
Dobrogea
Orogen
45 00N
Moesia
South Dobrogea
IMF
26 30E
27 30E
2500
2250
2000
1750
1500
1400
1300
1200
1100
1000
900
800
700
600
500
450
400
350
300
250
200
150
100
70
50
30
20
10
0
Seismicity
crust <20km
crust >20km
mantle <70km
mantle >70km
2
Mw
7

Figure 3

Focşani basin [*Matenco et al.*, 2003]. The pre-Neogene evolution and paleogeography of the Moesian platform is still a matter of debate [see *Pharaoh*, 1999; *Vaida et al.*, 2005]. Independently of this debate, at least 2 extensional events are well documented: a Permo-Triassic [*Răbăgia and Tărăpoancă*, 1999] and an early to middle Miocene events [*Răbăgia and Matenco*, 1999; *Tărăpoancă et al.*, 2003]. Reheating during these events led to a young thermotectonic age (<25 Ma), resulting in weak rheological characteristics [e.g., *Cloetingh et al.*, 2004].

[15] The North Dobrogea orogen, inserted between Scythian and Moesian platform SE of the front of the Carpathians contains remnants of a Variscan orogenic belt [e.g., *Săndulescu*, 1984], subsequently rifted during Late Permian–Early Triassic and inverted during the Late Triassic and Early Cretaceous times [e.g., *Seghedi*, 2001, and references therein]. This evolution resulted in a thick crust (~45 km [*Rădulescu*, 1988]) and presumably strong mechanical characteristics.

2.3. Continental Collision in the East Carpathians

[16] The "soft-collision scenario" that characterizes the East Carpathians occurred when the nonthinned parts of the lower plate entered the convergence zone. The last deformation along the sole thrust related to this collision is late Sarmatian in age (~11 Ma) and predates the latest Miocene to Pliocene posttectonic cover [see *Matenco and Bertotti*, 2000].

[17] In the northern part, shortening and collision with the East European/Scythian block was coupled with the foreland [*Ziegler et al.*, 1995], which was therefore affected by thrust faults paralleling the orogenic front [*Tărăpoancă et al.*, 2003]. This coupling has led to ~5 km of uplift and erosion in the orogen between 15 and 12 Ma [*Sanders et al.*, 1999]. Postcollisional sedimentation (post-11 Ma) in the lower plate is minor, and continuing low-scale rebound maintains the area geomorphologically stable at 200–300 m (Figure 3) [see also *Rădoane et al.*, 2003].

[18] Collision with the Moesian block in the southern part is characterized by a lower amount of orogenic shortening [*Matenco and Bertotti*, 2000] and minor orogenic uplift/erosion as inferred from fission track studies [*Sanders et al.*, 1999]. Recent studies on the 13 km deep, Neogene Focşani basin [*Tărăpoancă et al.*, 2003, 2004] demonstrated that it was affected by NW–SE oriented extension during middle Miocene (Badenian) times, i.e., in a direction perpendicular to the orogenic trend. Although the extension had limited values (stretching factors 1.1–1.2), this reduced the lithospheric strength and induced an additional thermal-derived load to the lower plate [*Tărăpoancă et al.*, 2004], besides the pull-down generated by the Vrancea slab [see also *Wortel and Spakman*, 2000].

2.4. Postcollisional Latest Miocene–Quaternary Basin Evolution

[19] Since the beginning of the Oligocene, the large Tethys basin started to divide into several subbasins in the Alps-Carpathians realm due to active mountains building processes. The Miocene tectonic events in the Carpathians generated further fragmentation of the northern Paratethys basin by producing a western (Transylvania and Pannonian basins) and an eastern basin (Dacic/Black Sea/Caspian basins), respectively. These semi-isolated basins characterized by brackish to freshwater sediments contain endemic faunas, with occasional connections to the main Tethyan realm [e.g., *Papaianopol et al.*, 1995; *Rögl*, 1996]. The Dacic basin represents the westernmost part of the Eastern Paratethys, developed during the postcollisional late Miocene (Sarmatian)–Quaternary time interval. Spatially, it is juxtaposed over the Moesian platform, overlying external orogenic nappes in case of the South Carpathians and the foredeep prolongation of the North Dobrogea orogen [see also *Jipa*, 1997; *Vasiliev et al.*, 2004] (Figure 1a).

[20] The NE-most part of the Dacic basin is juxtaposed with the Focşani basin, where subsidence increased during the postcollisional period, resulting in the deposition of up to 6 km of Pliocene to Quaternary lacustrine and continental sediments shed from predominantly Carpathian source areas [*Jipa*, 1997]. The sedimentary facies in the Dacic basin indicates mass progradation structures with nearshore facies, and large-scale deltaic environments developed especially during Pontian–lower Dacian times [*Jipa*, 1997]. The latter is a direct result of a generalized sea level drop (Messinian crisis) observed both in the Dacic basin [*Clauzon et al.*, 2005] and in the Black Sea [*Gillet et al.*, 2003]. As a result, the Dacic basin was gradually filled, during the early Quaternary only the central part of the Focşani basin remained lacustrine, alluvial sedimentation dominating elsewhere [see also *Jipa*, 1997; *Necea et al.*, 2005].

[21] Previous studies suggested that up to 2 km of Quaternary deposits accumulated in the Focşani basin [e.g., *Ghenea et al.*, 1971; *Lăzărescu et al.*, 1983] (Figure 4a). The

Figure 3. Digital elevation model of the foreland of the SE Carpathians with location of the Pliocene-Quaternary fault system depicted by the present study and the seismicity of the SE Carpathians. The 30 m resolution digital elevation model (DEM) was obtained through extraction and orthorectification of remote sensing Terra ASTER band 3 stereopairs [e.g., *Toutin*, 2002], and absolute tie points are from local topographic maps and the SRTM database [*Rabus et al.*, 2003]. Note the high topographic elevations of the lower Pleistocene (compare with Figure 2). Earthquakes and fault mechanism solutions are from the Romanian National Institute for Earth Physics (NIEP) database [e.g., *Radulian et al.*, 2002]. Separation in depth between crustal and mantle earthquakes was done using the crustal thickness map of *Merten et al.* [2005]. The dashed gray line represents the projection direction for the subcrustal earthquakes into the cross section displayed in Figure 13. Note that focal mechanisms solutions are given for crustal earthquakes only! For an overview of the well-known solutions of the intermediate-depth earthquakes, see, for example, *Oncescu and Bonjer* [1997]. See Figure 1 for location and text for further descriptions.

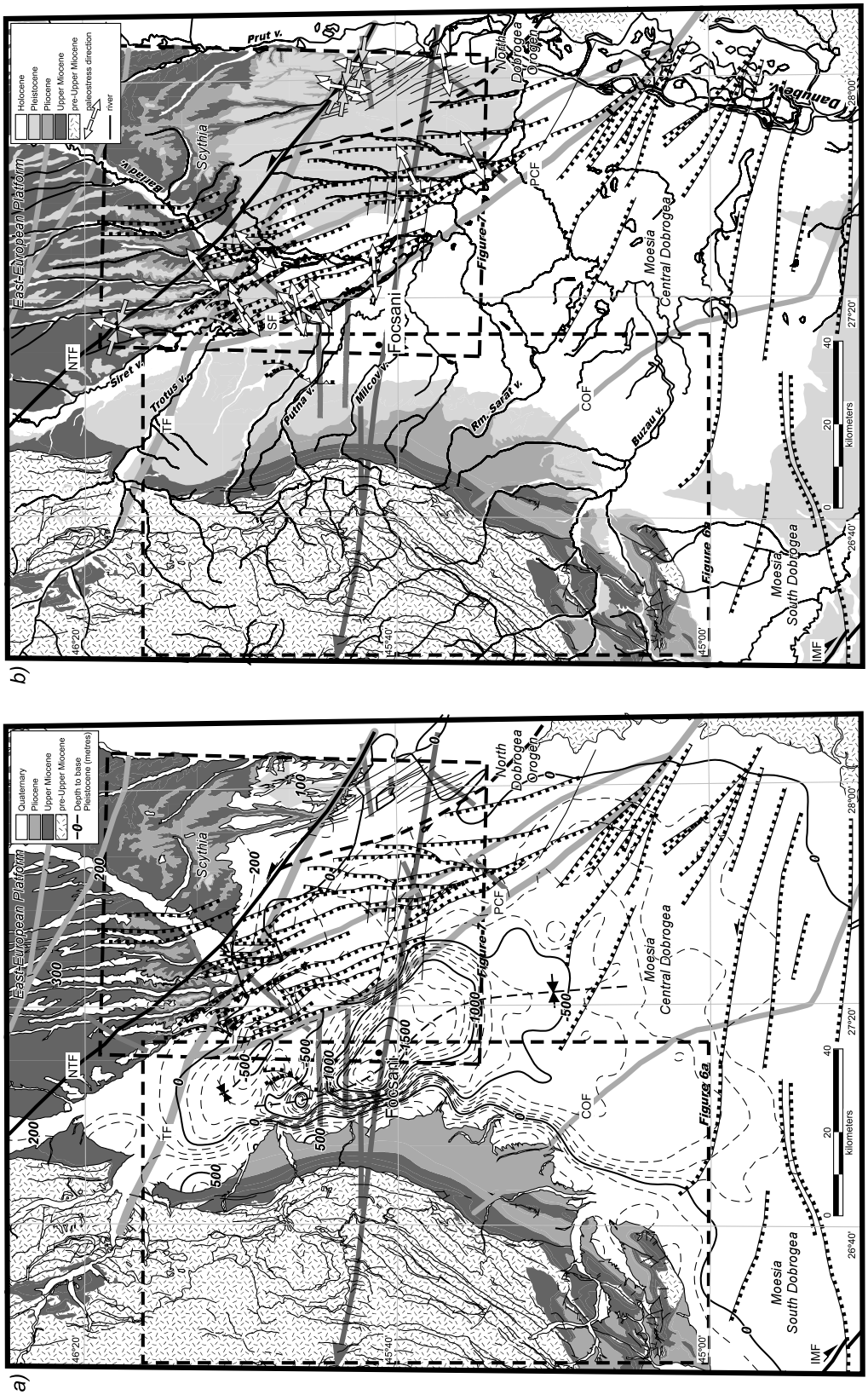

Figure 4. (a) Simplified geological map of the foreland of the SE Carpathians with the contours of the base of the Quaternary sediments. The map has been obtained through interpretation of regional seismic lines and 15 deep correlation wells, courtesy of Forest Oil International, SNP Petrom SA, and Rompetrol SA. Note the ~2 km depth of the Quaternary in the center of Focşani basin and the 500 m height in average elevation on the western flank. The location is given in Figure 1. (b) Simplified geological map of the SE Carpathians foreland with the location of the present-day river network and the paleostress axes calculated for the Quaternary deformation on the eastern Focşani flank. The latter were plotted as (sub)horizontal maximum (convergent) and minimum (divergent) principal axes directions of the restored stress field. See also *Matenco and Schmid* [1999] for further details regarding the field methodology. Fault abbreviations are as in Figures 1 and 2. The location is given in Figure 1.

lower Pleistocene is characterized by massive 400–1000 m thick gravels and conglomerates with thin interbedded clay and sandstone, known as the Candesti formation. By middle Pleistocene times, deposition of lacustrine levels of sands and gravels is gradually replaced by massive deposition of loess, distributed along several intervals from the flanks toward the center of Focşani basin, where the fluviatile sedimentation dominates the Holocene time interval [e.g., *Necea et al.*, 2005].

[22] Geomorphological analysis of present-day river profiles indicates a stable character of the river network north of the Trotus fault, reflecting the late Miocene collisional deformation. However, southward the fluviatile system is still uncompensated and unstable and clearly of younger, i.e., late Pliocene–Pleistocene age [*Rădoane et al.*, 2003]. Furthermore, surface transport models based on the present-day distribution of the sediment load of the major rivers infer a strong discrepancy between the erosion-sedimentation balance found north and south of the Trotus and Peceneaga-Camena fault systems, respectively [*Cloetingh et al.*, 2003] (Figure 2).

2.5. Vrancea Seismicity and GPS Measurements

[23] A large number of earthquakes concentrate in the SE Carpathians, focused in the so-called Vrancea area (Figure 3). The volume of 80 × 40 × 210 km intermediate-depth seismicity has been the subject of numerous studies [e.g., *Oncescu*, 1984; *Oncescu and Bonjer*, 1997; *Wenzel et al.*, 1999; *Gusev et al.*, 2002; *Bâlă et al.*, 2003, and references therein]. Fault plane solutions indicate vertical elongation of the seismically active volume [e.g., *Oncescu and Trifu*, 1987; *Oncescu and Bonjer*, 1997] at a high strain rate of 2×10^{-7} yr^{-1} [*Wenzel et al.*, 1999]. This is interpreted in terms of slab-pull exerted by subducted oceanic lithosphere forming the positive anomaly identified by seismic tomography studies [e.g., *Wortel and Spakman*, 2000; *Martin et al.*, 2006].

[24] In contrast with the intermediate-depth seismicity, less is known regarding the mechanisms of crustal seismicity and its relationship with the Pliocene-Quaternary deformations. Crustal epicenters concentrate along the Focşani basin flanks (Figure 3) and focal mechanism solutions do not provide a coherent crustal stress regime: they are dispersed and indicate compression and strike slip on the western Focşani flank and extension on its eastern flank.

[25] GPS measurements in the SE Carpathians [*van der Hoeven et al.*, 2005] demonstrate a ~3–4 mm yr^{-1} horizontal motion toward the SE of a Moesian block laterally bounded by the Intramoesian and Trotus Faults, postseismic deformation linked to the large Vrancea earthquakes being minor [e.g., *Vermeersen et al.*, 2004]. Preliminary results of the vertical GPS component (Figure 1a) show the existence of alternating domains of uplift and subsidence along a NW–SE oriented corridor. Note that these preliminary interpretations of the vertical component have large error bars, often larger than the values themselves (grayed in Figure 1a). These values were considered in our interpretation only if classical geodetical measurements *Popescu and Dragoescu*, 1986 are in agreement with the same order of magnitude. In addition, the distances between them are often too large to be directly correlated with geological units. On the overall, the subsiding areas coincide with places where young Pliocene-Quaternary basins are located, i.e., the Focşani (average 2–4 mm yr^{-1} up to 7.39 mm yr^{-1} GPS) and Braşov/Tîrgu (Tg). Secuiesc (−2.23 mm yr^{-1} GPS and 0–0.5 mm yr^{-1} geodetic) basins (Figure 1a). Although the later display a certain degree of noncorrelation, the fact that the Braşov basin was under subsidence during the Holocene was demonstrated by geomorphologic observations [*Posea*, 1981]. Uplifting areas are found south and NE of the Persani Mountains (~3 mm yr^{-1} GPS), the North Dobrogea (~2 mm yr^{-1} GPS and 1–2 mm yr^{-1} geodetic) and the frontal parts of the East Carpathians nappe pile (~1.5 mm yr^{-1}) (Figure 1a). The uplift is compatible with a very young age of uplift of the orogenic chain in the SE Carpathians, i.e.,<5 Ma [*Sanders et al.*, 1999], while the subsidence in the Focşani basin of 2–4 mm yr^{-1} corresponds to its ~2 km thickness of Quaternary deposits (Figure 1b). For details concerning the time series and its error bars we further refer to *van der Hoeven et al.* [2005].

3. Latest Miocene to Quaternary Structures in the Focşani Basin

[26] The Focşani basin contains uppermost Miocene to Quaternary beds, partly overlying the frontal parts of the Subcarpathian nappe and partly unconformably deposited over the older sequences of the Moesian platform (Figure 1b).

[27] The subsidence patterns in the center and their relationship with flank uplift were analyzed by interpreting recent industry seismic reflection lines available across the entire basin. Seismic lines, isochrone and isopach maps were converted to depth using average interval velocities derived from 15 regional wells. This analysis provided the regional geometry of Quaternary sediments (Figure 4a) and enabled the correlation of structures mapped at the surface with apparently active ones visible in the seismic lines. This has been combined with a tectonic geomorphology study of the outcropping upper Quaternary sediments in order to derive the recent vertical movements and the overall recent geometry and evolution of the entire Focşani basin.

[28] Structural data has been collected in some 150 locations distributed in uppermost Miocene (Pontian)–Holocene deposits on the eastern flank and upper Miocene (uppermost Sarmatian) to upper Pleistocene deposits on the western flank (Figure 4b). Brittle structures such as fault striations, folds, tension joints, fault-related folds (fault propagation, drag folds), regional-scale faults have been analyzed in order to derive regional paleostress directions. In places where a sufficient number of faults related to particular stages of deformation were available, the data sets were processed using the inversion method of *Angelier* [1984, 1989]; for details about the methods used, see *Matenco and Schmid* [1999].

3.1. Overall Geometry of the Focşani Basin

[29] The structure of the Focşani basin is that of a double plunge syncline, both flanks are deepening toward an ill-

defined axis located at ~30 km in front of the outcropping parts of the orogen (Figure 4a). The syncline is asymmetric. In the west strata gradually increase dip, up to a subvertical orientation near the contact with the frontal thrust of the Subcarpathian nappe. In the east the inclined beds change back into the subhorizontal orientation found over the North Dobrogea unit (Figures 1a and 5a).

[30] The general two-dimensional geometry indicates a deep basin with continuous sedimentation throughout the Miocene-Pliocene. Few to almost no stratigraphic terminations (e.g., onlaps, top laps) defining sequential unconformities can be observed in the entire package (Figure 5a), suggesting that subsidence kept pace with shallow marine to lacustrine sedimentation. Distal onlaps associated with normal faults dipping toward the orogen are observed in the middle Sarmatian, suggesting foreland flexure during thrust loading. Sarmatian-Pliocene strata increase in thickness toward the orogen, implying a farther westward located depocenter; hence the postnappe emplacement Focşani basin was extending westward of the present contact with the orogen, overlying the frontal exposed thrust [see also *Leever et al.*, 2006]. Proximal and distal onlaps in the lower Quaternary deposits suggest onset of flank uplift on both limbs (Figure 5a).

[31] This geometry of the Neogene-Quaternary deposits is similar across the entire central and southern parts of the Focşani basin. Southward, the amplitude of folding decreases, and consequently also the dips observed near the frontal orogenic thrust. To the north, the central and eastern parts of the basin are affected by a Pliocene age normal fault with eastward dip that was inverted during Quaternary shortening (Figure 5b) which separates in few second-order folds the main Focsani syncline (Figure 4a). Its mechanism is documented by the wedge-shaped geometry of the Pliocene deposits with hummocky reflections observed near the fault plane and tilted onlaps in the distal parts (Figure 5b), i.e., syntectonic deposits associated with a normal fault [e.g., *Prosser*, 1993]. Inversion is partial, the null point being located within Pliocene deposits [cf. *Williams et al.*, 1989]. To the north, inversion and offset gradually cease, and the normal fault offset is splayed into three to four smaller structures [see also *Leever et al.*, 2006]. The relatively rapid change in fault kinematics along strike (Figures 2 and 3) indicates that deformation reflects local accommodations in the high-amplitude folded areas of the Focşani syncline rather than regional events.

[32] The overall Quaternary Focşani basin axis strikes NNW–SSE and discordant to preexisting N–S oriented structures affecting the latest Miocene–Pliocene strata (Figure 4a). The deepest part of the Quaternary strata (~2 km) lies in the central area, where the distance between the orogenic front and the Peceneaga-Camena fault, i.e., the NE edge of the Moesian platform, is relatively small. As this distance increases southward (Figure 4a), the amplitude of the syncline gradually decreases to values of 50–100 m.

[33] The northern margin of the Quaternary Focşani basin is connected to a NW–SE oriented, subvertical fault, referred to as "New Trotus Fault" since it splays off the older Trotus fault toward the Carpathian orogen (NTF, Figures 2 and 3). Near the orogen, this fault is located ~30 km farther north of the pre-Neogene Trotus Fault. In the NW, the NTF displays the negative flower structure pattern (Figure 5c). An initial 1200 m of Sarmatian age vertical offset accommodating the gradual deepening of the southern sector, is associated with syntectonic deposits, and was subsequently reactivated during the Quaternary. A sinistral component of offset for tectonic events is proven by associated faults found in outcrops (stereoplot in Figure 5c), offsets of topographic and stratigraphic markers (latest Miocene-Pliocene strata on the topographic highs in Figure 3), and by the correlation with its effects on the neighboring thin-skinned nappe pile [*Matenco and Bertotti*, 2000]. Transtensional offset(s) (e.g., Figure 5c) and syntectonic sedimentation decrease toward SE from a maximum of ~5 km in map view near the nappe pile to ~100 m eastward. The changeover takes place where Moesia replaces the North Dobrogea orogen in the southern block of the NTF (Figure 2).

[34] Immediately to the NW of the New Trotus Fault, the geomorphology indicates uplift postdating the regional deposition of the lower Quaternary. This is observed through valleys incising through the entire stratigraphic section; lower Quaternary lacustrine gravels to fine clastics are found on top of the hills, at ~150 m elevation from the base level of the rivers (Figures 2 and 3).

3.2. Compressional Features at the Western Flank and Contact With the Thrust Front

[35] The contact between the external Subcarpathian nappe and the western flank of the Focşani basin is a key area for the study of postcollisional deformation in the foreland of the SE Carpathians. Interpretation of an industry seismic line which crosses the contact between the two units (Figure 5d) shows clear high-amplitude reflectors in the Focşani basin part of the section. These reflectors show a progressive increase in basin strata dip, from an average of 10° in the lower Quaternary (Figure 5a) to a subvertical orientation in the uppermost Miocene strata (Figure 5d). Again, no syntectonic patterns can be observed in the entire uppermost Miocene–Pliocene sequence (see Figure 5e for a correlation between Tethys and Paratethys ages), strata increasing in thickness westward, demonstrating that folding postdates the Pliocene. This seismic sequence is cut by the easternmost thrust, late Miocene (Sarmatian) in age, of the Subcarpathian nappe exposed at the surface, whose internal structure shows reflectors that dip to an opposite, i.e., westward direction. Although the deeper parts of the seismic line are less clear, it is certain that the continuous and high-amplitude reflectors of the basin unconformably overly an older thrusted sequence at larger depths (>10 km). This deeper thrust front represents the buried part of the Subcarpathian nappe formed also in late Miocene times. Higher-amplitude reflectors in this part of the line, assumed to be of Paleogene age [see also *Dicea*, 1995], help to separate the overlying lower Miocene strata from the individual thrust sheets.

[36] The most spectacular structure is the young high-angle reverse fault which postdates nappe emplacement and

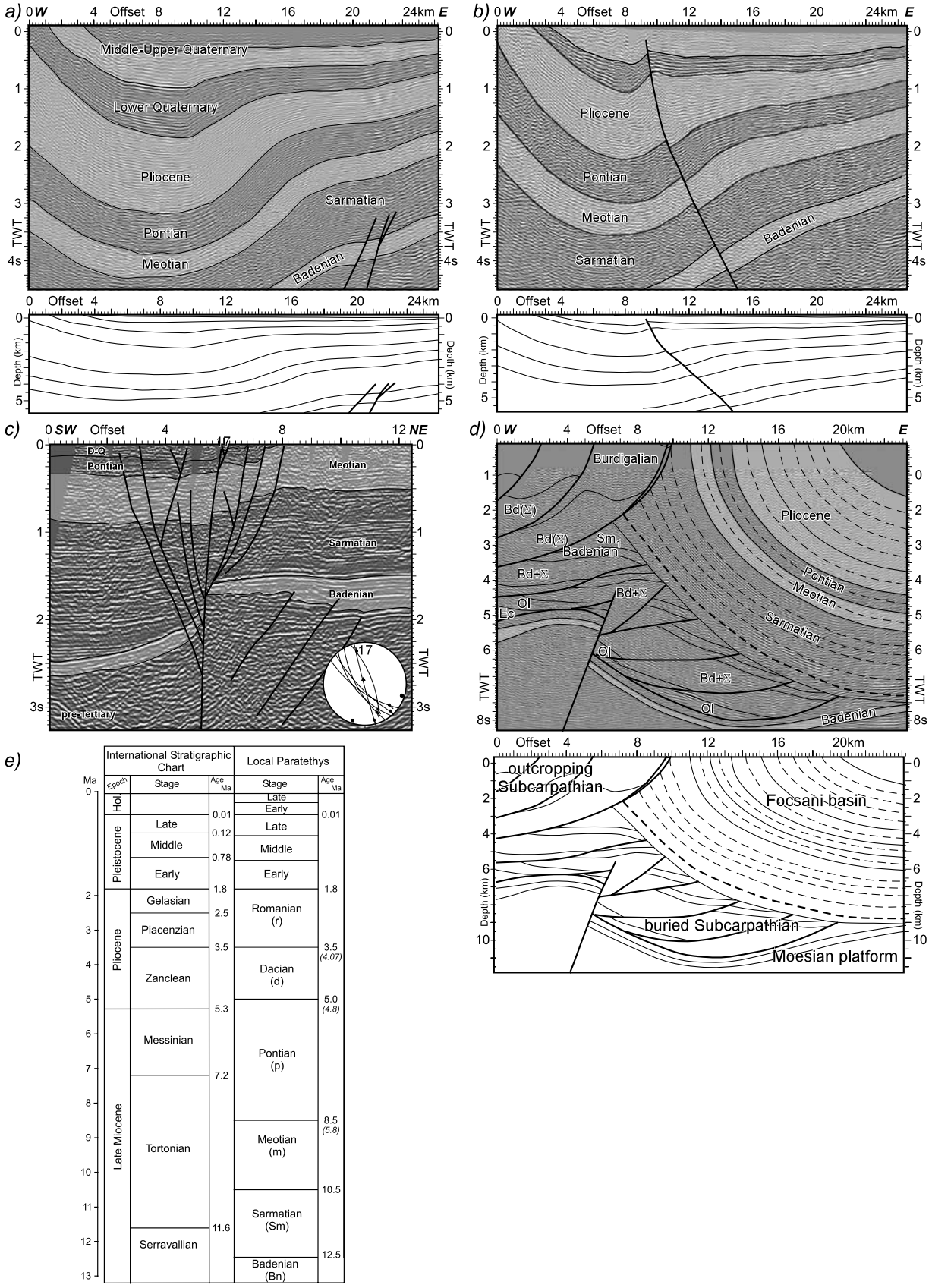
a)
Middle-Upper Quaternary
Lower Quaternary
Pliocene
Sarmatian
Pontian
Meotian
Badenian
TWT
Depth (km)
b)
Pliocene
Pontian
Meotian
Sarmatian
Badenian
c)
Q
Pontian
Meotian
Sarmatian
Badenian
pre-Tertiary
17
d)
Burdigalian
Bd(Σ)
Sm
Badenian
Bd+Σ
Ol
Ec
Pliocene
Pontian
Meotian
Sarmatian
outcropping
Subcarpathian
Focsani basin
buried Subcarpathian
Moesian platform
e)
International Stratigraphic Chart
Local Paratethys
Epoch
Stage
Age Ma
Holocene
Pleistocene
Late
Middle
Early
Gelasian
Piacenzian
Pliocene
Zanclean
Messinian
Late Miocene
Tortonian
Serravallian
Romanian (r)
Dacian (d)
Pontian (p)
Meotian (m)
Sarmatian (Sm)
Badenian (Bn)

Figure 5

formed coeval with the folding of the Focşani syncline. In this zone with less coherent reflectors the seismic interpretation is based on seismic facies correlation between foreland platform and nappes, on the truncation of reflectors and a correlation with the same structure as detected by tomographic inversion of the first arrivals from the Dacia-Plan reflection experiment [*Bocin et al.*, 2005]. Earlier studies [e.g., *Roure et al.*, 1993; *Matenco and Bertotti*, 2000] inferred a triangle zone at the contact between the Focşani depression and the orogen, whereby a large-scale back thrust supposedly accommodated uplift and folding of the strata in the Focşani basin. The seismic line indicates no reflectors truncation in the place where such a structure was inferred. We cannot completely exclude bedding-parallel backthrusting, but if present it must predate both Quaternary age folding in the Focşani basin and late Miocene thrust emplacement of the exposed Subcarpathian nappe units (Figure 5d).

[37] The surface expression induced by the folding of the western Focşani flank very directly demonstrates recent to active tectonics. A cross section along the Putna valley (Figures 6a and 6e) exposes progressively older strata when going from east to west: middle to upper Pleistocene dip 5–10° eastward, the dip change to 35° within the upper Pliocene (Romanian) (Figure 6b), then to 60° within the lower Pliocene (Dacian) (Figure 6c) and finally to subvertical (70–85°) within the uppermost Miocene (Meotian-Pontian) (Figure 6d). The middle to upper Pleistocene loess forms a smooth monocline, that can be followed along the entire western basin flank from the Trotus to the Buzău valley (Figure 6a) and which is crosscut by a younger W–E directed river network [see also *Fielitz and Seghedi*, 2005]. In the Putna valley, the loess sits on top of ~1 km thick and well stratified uppermost Romanian?–lower Pleistocene Candesti gravels. These gravels are known to be present in the subsurface of the entire SE Carpathians foreland. The coarse character of these sediments is rarely met in the syntectonic and posttectonic deposits of the deformed Carpathians units and reflects a major tectonic uplift in the westerly adjacent nappe pile and/or a climatic event [see also *Necea et al.*, 2005].

[38] The elevation of the base lower Pleistocene increases along the western flank from about −2 km in the basin center to an average of 600 m (maximum 996 m on the Odobesti hill) over a horizontal distance of 15 km (~17° average dip). The contact between the lower Quaternary gravels and the underlying Miocene-Pliocene basement is partly conformable, partly discordant. North of Putna valley the base Quaternary gravels were discordantly deposited onto sediments as old as the uppermost Miocene (Figure 6a). South of this valley, a conformable contact is demonstrated both by the reflection seismic lines (Figure 5a) and the gradual increase in dip seen in the field. This can be explained with the spatial position of two structural axes: the subsidence axis of the late Miocene–Pliocene sediments on the one hand and the folding axis in respect to Quaternary age (synclinal) folding on the other hand. These two axes coincide south of Putna valley, while farther north the axis of Quaternary folding diverges and approaches the orogen, probably as a result of strike-slip movements along the New Trotus Fault.

[39] A large number of uppermost Pleistocene–Holocene terraces can be observed in the field (Figures 6b and 6f), their elevation from the river base level increasing westward. Their analysis indicates two coupled and quantifiable uplifting events which occurred at the end of the early Pleistocene and during the middle to upper late Pleistocene, with an oblique trend in respect to the earlier late Miocene–Pliocene subsidence axis of the Focşani basin [*Necea et al.*, 2005].

[40] This overall image of the western Focşani syncline flank remains constant along strike toward the south until

Figure 5. Interpreted seismic profiles within the Focşani basin (locations in Figures 2 and 3). (a) Typical geometry of the Neogene deposits near the Quaternary depocenter of the Focşani basin. Note the relatively uniform patterns of the reflectors for the entire Miocene-Pliocene sequence. Two stages of syntectonic moments can be observed, based on the patterns of the reflectors (onlaps, wedge thinning), occurring during the lower and uppermost parts of the Quaternary. Abbreviations of the Paratethys ages are as in Figure 5e. (b) Interpreted profile in the central to northern part of the Focşani basin. Note the Quaternary age inversion of a Pliocene normal fault in the central part of the profile. This inversion is observed across the Pliocene synextensional sediments, massive wedge type of seismic facies near the fault surface, and the opposite offset for the pre- and post-Pliocene strata. (c) Interpreted seismic profile crossing the New Trotus Fault. Note the negative flower structure and the two syntectonic packages, Sarmatian (thickness variations) and Quaternary (fault offsets). The stereoplot represents faults with sinistral sense of movement observed at surface, in the immediate vicinity of the main fault (location in Figure 7). In Figures 2 and 3 only, the main fault has been drawn. (d) Interpretation of a seismic profile crossing the contact between the exposed part of the Subcarpathian nappe and the Focşani basin. Note the overall synclinal shape of the basin, subvertical orientation of the strata in the western flank, indicating that the basin was extending farther westward, covering the external nappe pile prior to the Quaternary. The thick dashed line represents the potential position of a frontal back thrust inferred by previous studies [e.g., *Matenco and Bertotti*, 2000]. Note that the main deformation age of the frontal outcropping thrust is late Miocene (Sarmatian). An additional 1.5 km thrust offset during the Quaternary has also been suggested by previous restorations [*Leever et al.*, 2006]. For further descriptions, see text. (e) Correlation between the standard Tethys and Eastern Paratethys ages used in the present study. The absolute ages follow the correlation of *Rögl* [1996], except the Sarmatian boundaries, which are drawn after *Mărunţeanu and Papaianopol* [1995]. Ages in italics are the absolute values obtained by the magnetostratigraphy study of *Vasiliev* [2006].

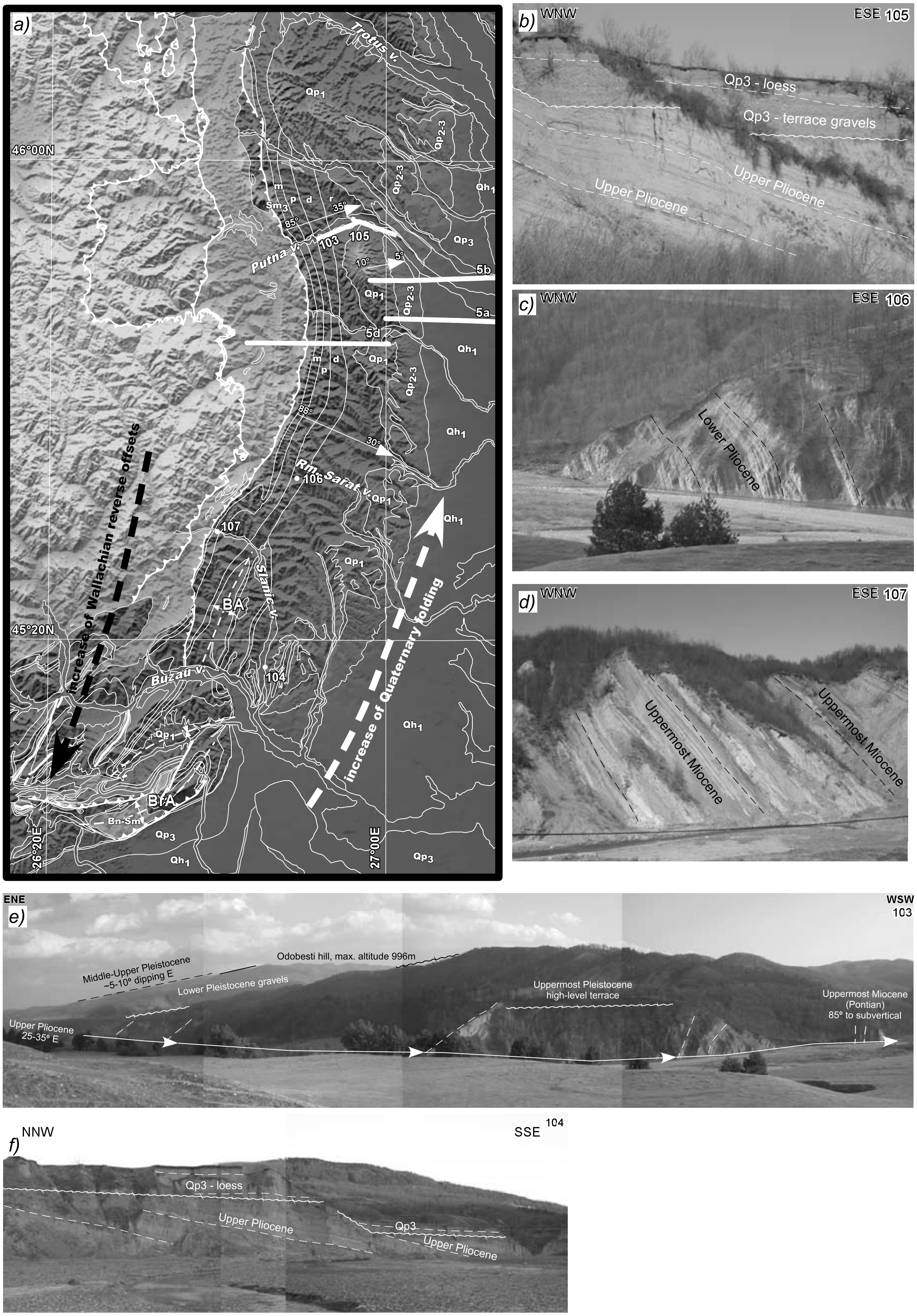
a)
Trotus v.
Qp1
46°00N
Qp2-3
Qh1
m
Sm3
p
d
r
35°
85°
Putna v.
103
105
10°
5°
Qp3
5b
5a
5d
88°
30°
Rm. Sarat v.
106
107
Slanic v.
BA
45°20N
Buzau v.
104
increase of Wallachian reverse offsets
increase of Quaternary folding
BrA
Bn-Sm
26°20E
27°00E
b)
WNW
ESE 105
Qp3 - loess
Qp3 - terrace gravels
Upper Pliocene
Upper Pliocene
c)
WNW
ESE 106
Lower Pliocene
d)
WNW
ESE 107
Uppermost Miocene
Uppermost Miocene
e)
ENE
WSW
103
Odobesti hill, max. altitude 996m
Middle-Upper Pleistocene
~5-10° dipping E
Lower Pleistocene gravels
Uppermost Pleistocene
high-level terrace
Uppermost Miocene
(Pontian)
85° to subvertical
Upper Pliocene
25-35° E
f)
NNW
SSE 104
Qp3 - loess
Upper Pliocene
Qp3
Upper Pliocene

Figure 6

the region of the Buzău valley, where a second-order anticline (i.e., the Berca anticline) marks the transition toward the typical area for which NW–SE oriented (Pliocene?) Quaternary (Wallachian) contraction was first documented [e.g., *Hippolyte and Săndulescu*, 1996], in the form of the Breaza anticline (Figure 6a).

3.3. Quaternary Extension and Strike Slip Along the Eastern Flank

[41] Along the entire eastern Focşani flank a large number of faults with offsets of up to 200 m truncate the upper Quaternary sediments with associated topographic offsets. Because of this truncation and in view of the shallow crustal seismicity observed along the fault planes (Figure 3) faulting is considered as presently active (Figures 7–11). The faults truncate an uppermost Miocene to Pliocene alternation of clastics, 2–20 m thick lower Pleistocene gravels and <20 m of middle-upper Pleistocene loess deposits (Figure 2).

[42] The surface expression of these faults have various (geo)morphological characteristics. Uplifted topographic linear cliffs (footwall) often delineate lowland areas (hanging walls) along the strike of the normal faults (Figures 8b, 8c, 8e, and 9d). Offsets in the Pliocene basement clastics by centimeters to meters create weakness zones along which the exposed middle-upper Pleistocene loess suffered intense suffusion. As a result, canyons that are tens of meters deep formed in this loess at the surface, with lengths of kilometers and forming linear patterns (Figures 10d, 10f, 11b, 11c, 11d, and 11e). Although in theory such morphological phenomena may also be linked to other processes, such as thickness variations or change in composition, the offsets in the underlying basement observed in the ones used in this study to derive kinematics indicate a tectonic origin. The development of landslides, hundreds of meters to kilometers in length, is typical for faults with larger offsets in the order of tens of meters (e.g., Figures 9d and 9e).

[43] Two types of deformation features are recognized in this area. First, a large number of NW–SE to NNW–SSE oriented normal faults accommodates the gradual deepening of the Miocene-Quaternary sequence toward the center of the Focşani basin. Accommodation is achieved either over a large horizontal distance via a large number of normal faults with smaller offsets, as is the case in the NW sectors (Figures 8a and 9f), or alternatively, over a narrow horizontal distance involving a smaller number of normal faults with larger offsets, as is the case in the SE sectors (Figures 10a and 10b). The lateral transition between the two areas is either made through splaying of the normal faults toward the NW or through E–W transfer faults (see also Adjud fault [*Tărăpoancă et al.*, 2003]) (Figure 7). The second type of active deformation involves strike-slip faulting, mostly sinistral, and is widespread in the SE corner of the studied area. It is interpreted to be genetically linked to a horse tail termination of the offset produced along the New Trotus Fault (Figures 7, 10h, 11a, and 11f).

3.3.1. Normal Faulting Near the Moesia-North Dobrogea Transition

[44] The normal fault system along the eastern Focşani flank is clustered in the sediments covering the North Dobrogea unit, near or at the contact with the Moesian platform. The most apparent large-scale feature of the NE trending normal fault system is the Siret fault, which in plan view roughly coincides with the location of the pre-Neogene Peceneaga-Camena fault in its NE sector (Figures 2 and 7). It accommodates an uplift of the NE block and is clearly mapped at the surface (Figures 8b–8d). This fault represents the limit between two different structural domains regarding Quaternary deformation: the faulted North Dobrogea unit to the NE and the folded Moesian platform to the SW. It is associated with a topographic offset of 20–250 m along a (sub)vertical cliff (Figures 8b and 8c) decreasing from NW to SE. The latter separates the Pleistocene gravel and loess deposits in the 150–300 m high plateau of the North Dobrogea in the ENE from the WSW-ward adjacent upper Holocene alluvial and loess deposits found at an elevation of 5–50 m in the Focşani basin flatland (Figure 7). Two types of NNW–SSE oriented normal faults can be measured at the outcrop scale. High-angle (50–70°) normal faults root into the basement and consequently are of tectonic origin (WSW–ENE extension). Low-angle (20–30°) faults formed as a result of gravitational collapse of the cliffs (loess on top of gravels) (Figure 8d). The only available seismic line crossing the fault is located in an area where the offset is small (~20 m), close to the line resolution (e.g., Figure 8a).

Figure 6. Topographic expression of Pliocene-Quaternary tectonics on the western flank of the Focşani basin. (a) SRTM shaded DEM with overlying stratigraphic limits and major faults. Note the decreasing dip of the strata, from subvertical near the main thrust front to ~5° in the late Pleistocene (white arrows). The shape of the Focşani syncline is complicated by a second-order folding (Berca anticline BA) toward SSW. In the SW corner, the "Wallachian" phase thrusting is observed through ENE-WSW oriented folds and thrusts, in the area of Breaza anticline (BrA). South of this structure, a large thrust with 500 m offset divides the folded area from the flat-lying Holocene sediments on the Moesian platform. Note the unconformity between the lower Quaternary and older underlying strata NW of the Putna valley. The location is given in Figure 2. Numbers 103–107 are locations of Figures 6b–6f. Abbreviations of eastern Paratethys ages as in Figure 5e. (b) Alternation of upper Pliocene clastics, dipping ~25° eastward, covered by a high level latest Pleistocene terrace, made up of alluvial gravels and loess on top. (c) and (d) Highly inclined uppermost Miocene to lower Pliocene of the western Focşani flank. (e) Panoramic view of the western Focşani flank structure in the area of Putna valley. Note the Quaternary mountain (Odobesti Hill) and the change in dip westward. (f) Multiple terrace levels in the area of Slanic valley, covering upper Pliocene tilted sediments.

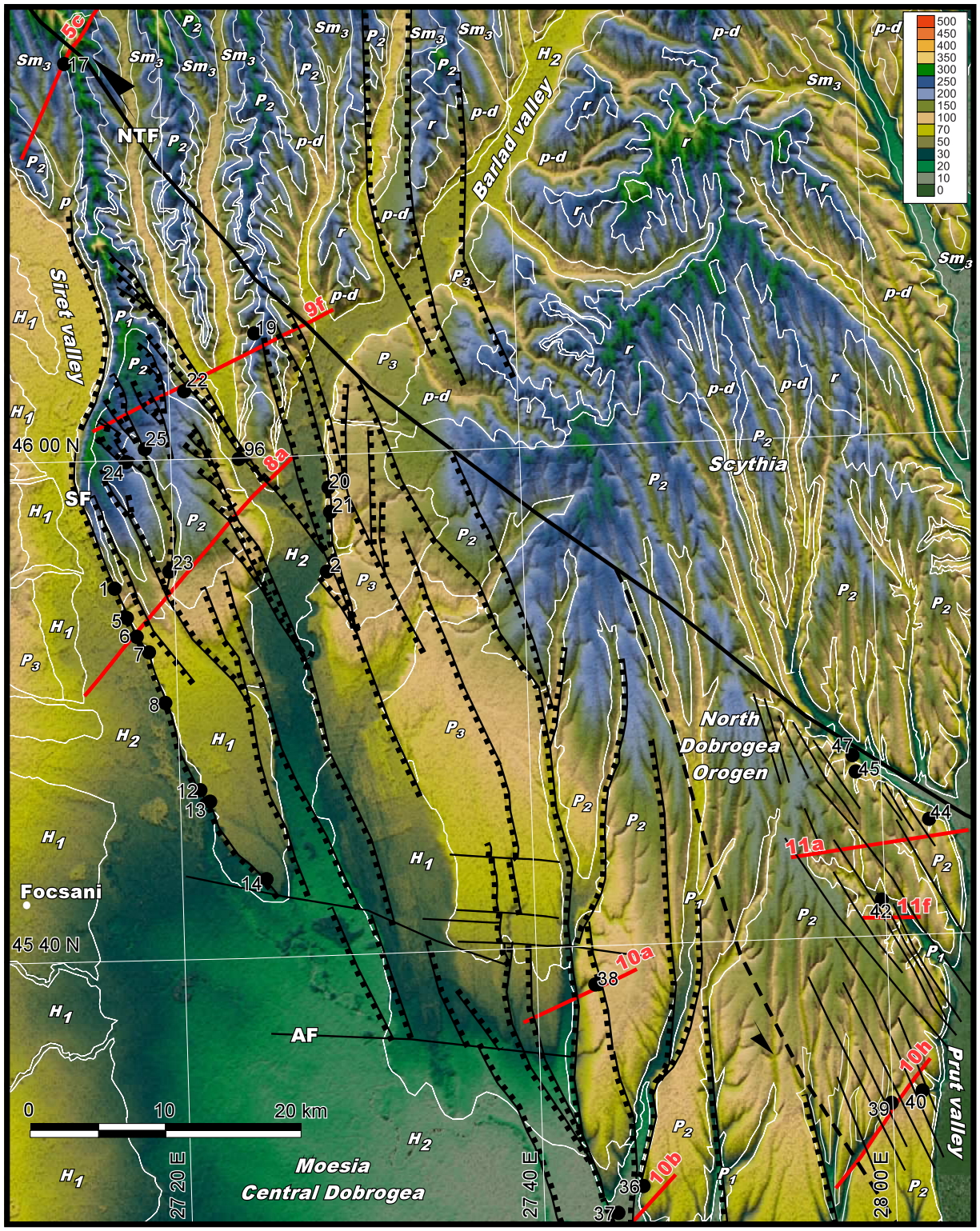
Sm3
P2
P3
P1
H1
H2
p-d
r
NTF
SF
AF
Siret valley
Barlad valley
Prut valley
Scythia
North Dobrogea Orogen
Moesia
Central Dobrogea
Focsani
46 00 N
45 40 N
27 20 E
27 40 E
28 00 E
0 10 20 km
5c
9f
8a
10a
10b
10h
11a
11f
500
450
400
350
300
250
200
150
100
70
50
30
20
10
0

Figure 7

[45] Other and smaller-scale normal faults are observed in the NW sector (Figure 7). Offsets by tens of meters are visible in topographic differences (Figure 8e) or through deep canyons (Figure 9b). The eastward dipping normal faults dominates, accommodating the overall deepening direction of the strata. Often, regional-scale conjugate faults can be mapped at the surface along synthetic-antithetic systems (Figures 9a, 9b, and 9c), confirmed by neighboring seismic lines (Figure 9f). Outcrop kinematics indicate offsets by centimeters to meters, commonly displacing the Pliocene clastics and the overlying lower Pleistocene gravels (e.g., Figures 8f and 8g). These outcrop faults are NW–SE oriented, apart from a few local deviations (such as NNE–SSW, Figure 8g).

[46] In the SW part of North Dobrogea orogen, a smaller number of normal faults can be mapped in the seismic lines, producing larger offsets in the order of hundreds of meters (Figures 10a and 10b). Spatially, they partly coincide with earlier (Badenian-Sarmatian) normal faults (Figure 10b). Adding up these offsets indicate up to 1.5 km deepening of the Moesian pre-Neogene basement with respect to its depth in the North Dobrogea orogen during the Neogene-Quaternary times. Reactivation of these normal faults and creates rollover anticlines involving syntectonic lower Quaternary sediments. Despite their clear signature in the upper parts of the seismic lines, these faults are poorly expressed by surface kinematics. Only a few landslides and canyons with offsets in the upper Pliocene (Figures 10c, 10d, and 10g) can be found in the field, possibly as a result a reduction of active deformation during the Quaternary.

3.3.2. Strike-Slip Deformation Along the Easternmost Portion of the (New) Trotus Fault

[47] Different Quaternary kinematics is observed for the faults in the easternmost part of the studied area (SE corner of Figure 7, west of the Prut river and south of the (New) Trotus fault, see also Figure 4). The Miocene-Quaternary deposits are thinner in comparison with the Focşani basin, because of a distal position in respect to both late Miocene foredeep flexure and postorogenic subsidence and folding. In seismic lines (Figures 10h, 11a, and 11f), barely visible (sub)vertical faults converge at depth into vertical faults and indicate flower structures (in most places negative). Few individual normal faults are also observed here (e.g., at the east and west margins of Figure 11a, west part of Figure 11f) but mostly subvertically oriented.

[48] Large canyons in the middle Pleistocene loess are observed at the surface (e.g., Figures 10 and 11), connected with the faults that truncate the Quaternary sequence. The large number of these faults with small offsets by meters indicates that deformation is rather distributed along a km wide fault zone without individual major structures, interpreted as reflecting horse-tail type of strike-slip termination of the New Trotus Fault. The faults display small (centimeters to meters) sinistral offsets in the underlying shaly Pliocene strata (Figure 10e) at the base of the up to 20 m deep canyons developed in loess deposits (Figure 10f). One exception exhibiting apparent transpression can be locally observed (Figure 10h, middle of the section). Reverse fault components organized within a formerly Sarmatian positive flower structure, were subsequently reactivated during the Quaternary with a normal component (transtension) and exhibiting sinistral kinematic indicators at the surface (e.g., Figure 10e).

[49] In regions situated in close proximity to the New Trotus Fault sinistral transtension is focused on a smaller number of very clear fault traces exhibiting higher offsets (Figure 11). Two flower structures can be defined in the seismic lines (Figures 11a and 11f), 30–40 m deep canyons dominate the loess topography (Figures 11b and 11d) with offsets of meters in the underlying Pliocene–lower Pleistocene basement. Entire hilly areas are traversed by active en echelon fractures (Figure 11c), obliquely oriented in respect with adjacent valleys, i.e., not reflecting drainage patterns. All morphological stages of canyon development are observed, from initial fracturing of the underlying basement (Figures 11c and 11g) toward subsequent exaggeration by loess suffusion along active fault planes.

[50] South of the Focşani basin, the active faults detected by interpretation of seismic lines and morphological markers indicate WNW–ESE to E–W oriented normal faults, accommodating offsets of up to 20–30 m of the base Quaternary. These faults are mostly synthetic in relationship with the direction of basin deepening, accommodating the northward increase in Quaternary thickness. Dextral components across the fault planes can only be guessed from the flower-type of the structures seen in seismic lines and displacements of strata.

4. Postcollisional Tectonic Evolution

[51] Previous latest Miocene to Quaternary (postcollisional) orogen and basin evolution studies demonstrated apparently contrasting styles of deformation and associated vertical movements in the area of the East and South

Figure 7. Detailed topographic expression of Quaternary and active faulting that takes place on the eastern flank of the Focşani basin. AF, Adjud fault [cf. *Tărăpoancă et al.*, 2003]; SF, Siret fault. Figure conventions are as in Figure 3. Note that the normal fault system developed at the Moesia–North Dobrogea transition, the strike-slip system developed in the eastern part, and the topographic offsets developed along the NW sector of the New Trotus Fault. The dashed line represents the separation between the normal and strike-slip systems and can possibly be interpreted as a reactivation of an older pre-Neogene lineament (limit between the North Dobrogea and the pre-Dobrogea depression, Scythian Platform, or internal limits into the North Dobrogea). Red lines and numbered black dots indicate the location of the seismic lines and paleostress measurements in Figures 8–11. The location is given in Figure 2. Sm3, upper Sarmatian; p, Pontian; d, Dacian; r, Romanian; P1, lower Pleistocene; P2, middle Pleistocene; P3, upper Pleistocene; H1, lower Holocene; H2, upper Holocene.

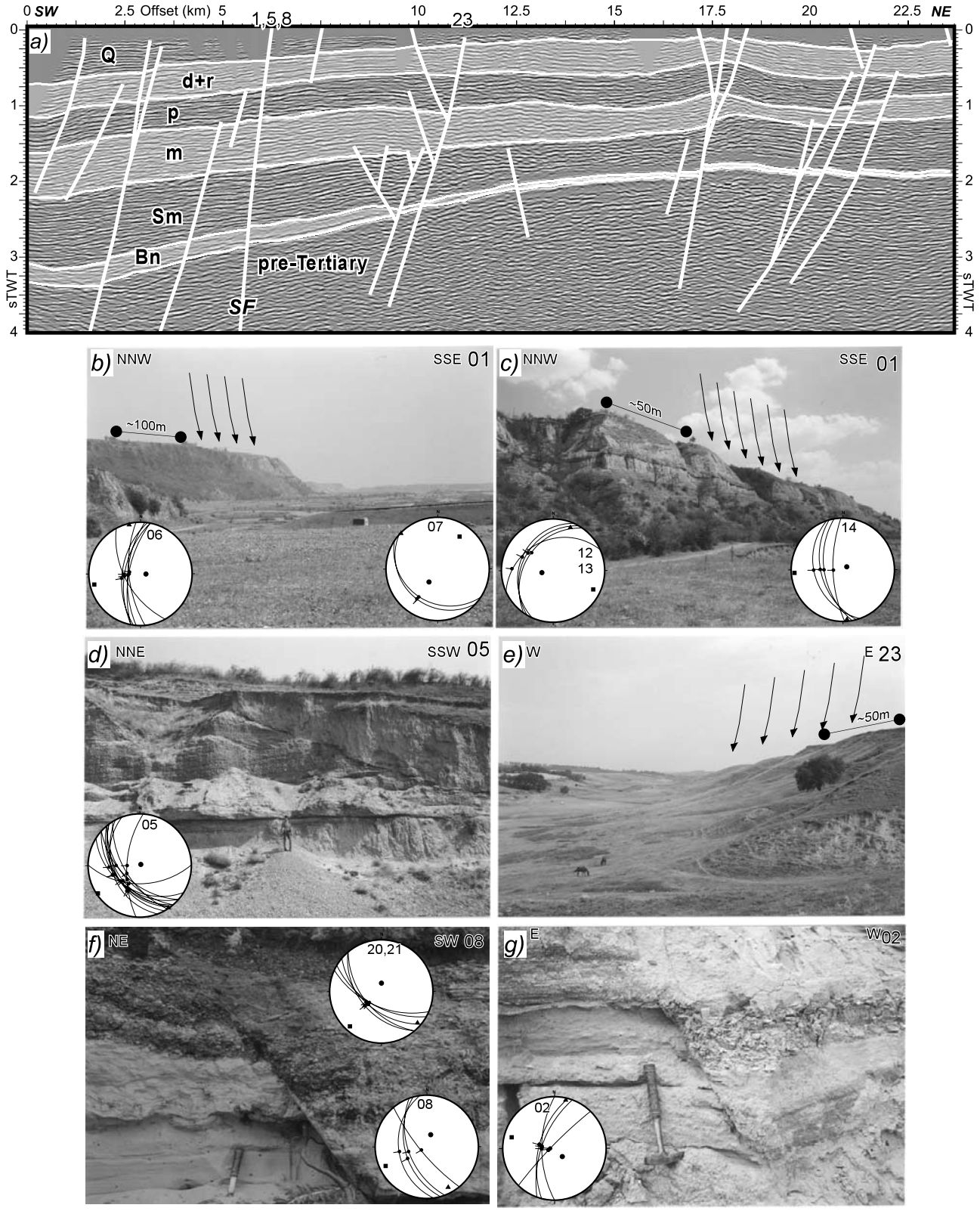
0 SW
2.5 Offset (km) 5
1,5,8
10
23
12.5
15
17.5
20
22.5 NE
a)
Q
d+r
p
m
Sm
Bn
pre-Tertiary
SF
sTWT
b) NNW
SSE 01
~100m
06
07
c) NNW
SSE 01
~50m
12
13
14
d) NNE
SSW 05
05
e) W
E 23
~50m
f) NE
SW 08
20,21
08
g) E
W 02
02

Figure 8

Carpathians foreland [e.g., *Matenco et al.*, 2003; *Bertotti et al.*, 2003]. Our study links these contrasting styles to a coherent process occurring at a regional scale. Two main tectonic phases are evident from the style of deformation. During a first late Miocene–Pliocene phase subsidence affected Moesia and the previously juxtaposed external Carpathian nappes. This was followed by a Quaternary age episode of contraction (Figure 12a). The second episode was only active in a WNW–ESE oriented corridor confined by the Intramoesian fault in the SW and the Trotus and Peceneaga-Camena faults to the north and NE (Figure 1).

4.1. Latest Miocene–Pliocene (Late Sarmatian–Romanian) Subsidence

[52] In this time interval subsidence is observed over the entire Moesian platform, i.e., from the (New) Trotus fault in the east and NE all the way to the Danube Gorges in the west, at the junction of the Carpathians with the Balkans. Spatially, the overall subsiding area coincides with the western part of the Eastern Paratethys, i.e., the so-called Dacic basin covering Moesia, partly Scythia and the buried part of North Dobrogea (Figure 1a). The subsidence magnitudes gradually increase from the Danube Gorges to the east and from east to west in the frontal part of the East Carpathians, sediments having a minimum thickness over the North Dobrogea orogen (e.g., Figure 11a) and attaining maximum values in the area of the Focşani basin. In the latter, two stages of subsidence can be observed on the basis of the width of the basin across the orogen (Figure 12a) [see also *Leever et al.*, 2006]. A first stage of latest Miocene (latest Sarmatian–Pontian) subsidence led to gradual burial of the frontal part of the East Carpathian nappes. The Messinian sea level drop [*Clauzon et al.*, 2005; *Gillet et al.*, 2003] during the Pontian [*Vasiliev*, 2006] cannot be observed in the Focşani basin, where sedimentation is continuous, keeping pace with ongoing subsidence. During the Pliocene, sedimentation extended as far west as the Braşov area and the easternmost parts of the Transylvania basin (Figure 1a). There the Pliocene (upper Dacian–Romanian) sediments have the same endemic biostratigraphy to that found in the Dacic basin, their geometry indicating a connection over the thrust nappes toward the foreland [e.g., *Marinescu and Papaianopol*, 1995; *Olteanu*, 2003].

[53] The sediments in the Focşani basin area point to rather continuous late Miocene–Pliocene tectonic subsidence (e.g., Figure 5). Hence the division into two stages of subsidence appears to be artificial in purely tectonic terms. It is created by the juxtaposition of an eustatic (Messinian) event at the end of the Miocene, well observed in other, shallower parts of the Dacic basin.

4.2. Quaternary Contraction

[54] Our data demonstrate Quaternary age coeval subsidence in the Moesian foreland and uplift of the external nappes of the SE Carpathians. Reduced Quaternary subsidence (<2–300 m) is also observed in the internal SE Carpathians, in the Braşov and Tg. Secuiesc basins [e.g., *Posea*, 1981; *Visarion and Rotaru*, 1988]. We interpret these features as a result of one tectonic event, i.e., contraction, and the couple uplift/subsidence as regional-scale folding observed by this study in the upper crust (Figure 12a). This is directly associated with ~2 km offsets high-angle reverse faulting truncating the basement below the external nappes (Figure 1b). The shortening does not reactivate the Carpathians sole thrust and therefore not orogenic-related.

[55] High resolution seismics [*Leever et al.*, 2006] and geomorphological interpretations [*Necea et al.*, 2005] have detected a folding wavelength of ~130 km and a foreland migration of the null point (zero vertical movement). This temporal migration explains why limited areas on the western flank of the Focşani basin (<20 km wide), initially in subsidence (synclinal folding with syntectonic patterns) at the beginning of the Quaternary (lower Pleistocene gravels) were inverted and uplifted to high topographic elevations during the second late Pleistocene folding event (Figure 12a). Coincidentally, the area covered by the normal faults collapse at the eastern flank of the Focşani basin has a similar width and spatially corresponds to the zone inverted from subsidence to uplift during Quaternary migration of the null point (Figure 12a).

[56] Quaternary contraction also caused the high-angle reverse faults in the core of the overall uplifting anticline formed by the external nappes. This is compatible with shallow high-velocity anomalies derived from seismic experiments pointing to an uplifted (4–8 km) position of the Moesian basement below the thin-skinned units (Figure 1b)

Figure 8. (a) Interpreted seismic profile across the eastern flank of the Focşani basin. The "1,5" marks the location of the Siret fault, visible in Figures 8b–8e and roughly juxtaposed onto the inferred pre-Neogene Peceneaga-Camena fault. Note the development of a Quaternary normal faulting system, generally dipping westward and associated with antithetic faults. Locally, this system inverts earlier faults (location "95"). SF, Siret fault. (b), (c) and (d) Outcrop expressions of the Siret fault with variable offset that increases from south to north, i.e., from ~20–30 m (Figure 8b) to ~150 m (Figures 8c and 8d). Kinematic structures are either linked normal faults observed on seismic sections or with gravitational structures formed due to cliff collapse (Figure 8d). (e) Morphological step-like expression of a normal fault detected at depth in the interpreted seismic line (Figure 8a, location "23"). (f) and (g) Outcrop-scale expression of the normal faulting. A clear offset of the interface between Pliocene-Pleistocene clastics and overlying loess is visible. Locations of seismic line and outcrops are given in Figure 7.

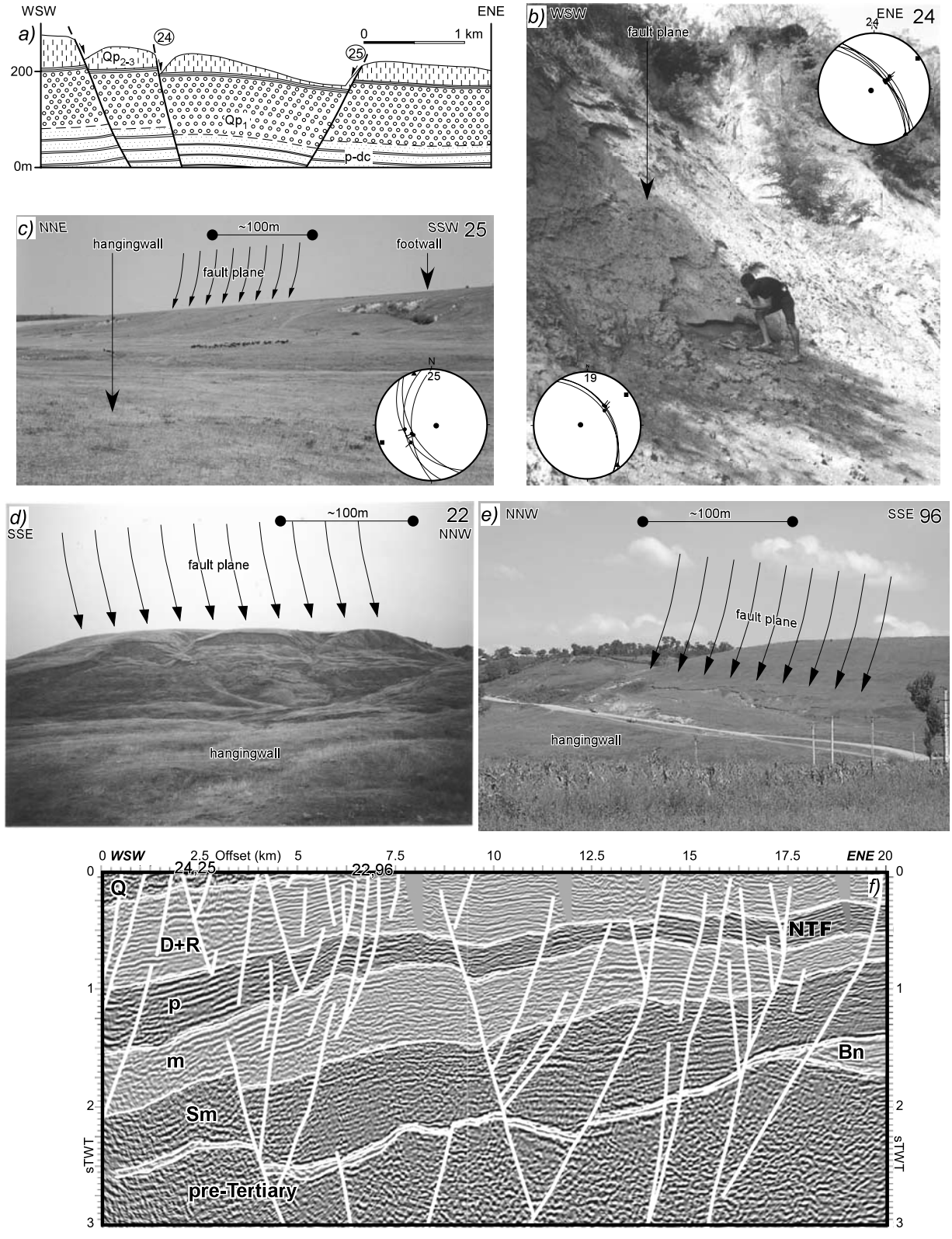
a)
WSW
ENE
24
25
0
1 km
200
0m
Qp2-3
Qp1
p-dc
b)
WSW
ENE 24
fault plane
24
c)
NNE
SSW 25
~100m
hangingwall
footwall
fault plane
N
25
19
d)
SSE
22
NNW
~100m
fault plane
hangingwall
e)
NNW
SSE 96
~100m
fault plane
hangingwall
0 WSW
2,5 Offset (km) 5
7.5
10
12.5
15
17.5
ENE 20
24, 25
22, 96
Q
D+R
p
m
Sm
pre-Tertiary
NTF
Bn
f)
sTWT
0
1
2
3

Figure 9

[see also *Landes et al.*, 2004; *Bocin et al.*, 2005]. A similar structure was also interpreted from surface geology [e.g., *Roure et al.*, 1993]. This is an accommodation structure in the core of the regional anticline (Figures 1a and 12a) and is not related to nappe emplacement. The foreland vergence of the anticline is suggested by the (sub)vertical orientation of the strata at the western Focşani flank (Figure 1b).

[57] The vertical amplitude of folding in the external nappes anticline is comparable to that of the Focşani syncline (~2 km, Figure 5). The uplifted external nappes anticline has a higher magnitude of 2–5 km, based on fission track evidence [*Sanders et al.*, 1999] and U-Th/He dating [*Merten et al.*, 2005].

4.3. Lateral Transfer of Quaternary Shortening

[58] The Quaternary shortening in the SE Carpathians and their foreland near the Focşani depocenter is in the order of 5 km [*Leever et al.*, 2006]. This amount needs to be transferred to other structures southward, i.e., toward the Valachian part of the Moesian platform (Figure 1a), which does not record Quaternary folding, but rather exhibits a much decreased continuation of the earlier Pliocene subsidence. The main change, and hence transfer, takes place reactivating the late Miocene (Sarmatian) dextral Intramoesian fault [e.g., *Matenco and Schmid*, 1999], which records 5 km dextral displacement during post-Miocene times [see also *Tărăpoancă et al.*, 2003].

[59] From the Intramoesian going eastward and northward, the amount of Quaternary shortening recorded by the Focşani syncline increases toward its depocenter, coinciding with a decrease in the amount of shortening recorded by the Wallachian thrusts (Figure 6a) along the same direction. These rather high-angle reverse faults [e.g., *Ştefănescu et al.*, 2000] have traditionally been assumed to be of Pliocene to Quaternary age [*Săndulescu*, 1988], but wherever timing constraints are available, Quaternary age sediments are always affected (e.g., Breaza anticline, Figure 6a). We interpret the Quaternary amplitude of the Focşani basin decreasing southward since shortening by folding is transferred toward the high-angle Wallachian reverse faults, which have a dextrally transpressive component [see also *Matenco et al.*, 2003] (Figure 6a).

[60] The 5 km shortening by folding created an ESEward movement of the Moesian block on which the Focşani syncline is juxtaposed (Figure 12b). This movement is not observed in the Scythian domain and caused a comparable sinistral offset along the New Trotus Fault. As the folding amplitude decreases eastward, the sinistral offset is reduced to a couple of hundreds of meters. The transtensional component of this fault is related to the contact with Moesia subsiding along the Focşani axis.

5. Inferences for the Lithospheric-Scale Mechanism

[61] Although our data are located in the upper crust, they do provide arguments for the lithospheric-scale mechanism responsible for the intermediate-depth anisotropy and Vrancea earthquakes. A number of hypothesis were proposed to explain these mantle features shifted toward the SE by ~100 km from the position of the tectonic unit known to contain an ophyolitic suture and/or associated sediments (Outer Dacides [e.g., *Săndulescu*, 1984]), i.e., the potential Wadati-Benioff zone [see *Knapp et al.*, 2005]. Most of the mechanisms assume time-dependent lateral processes acting in the Carpathians slab either across or along the orogen.

[62] The model of *Royden* [1993] associates the roll back of the subducting plate with deep foreland basins (e.g., Carpathians, Apennines). This model looks valid for the middle-late Miocene period until 11 Ma of Carpathians subduction/collision and coeval Pannonian back-arc collapse [e.g., *Fügenschuh and Schmid*, 2005]. However, it cannot explain the thick postcollisional sediments of the Focşani basin because roll back is active during subduction and necessarily stops after collision. A similar problem in timing is documented for the delamination model, either oceanic slab types [e.g., *Gvirtzman*, 2002] or continental [*Knapp et al.*, 2005]. A migration eastward of the lithosphere which is peeling off can be associated with delamination model [*Gîrbacea and Frisch*, 1998], but this should be associated near the surface with a migration of depocenters in particular across the strike of the orogen. This is an effect which is not observed, but on the opposite, the subsidence extended westward during the Pliocene reaching the Braşov basin [e.g., *Olteanu*, 2003; *Leever et al.*, 2006]. All these delamination or combined models have one upper crustal assumption, that extension in the Braşov basin due to asthenospheric/magmatic rise is coeval with frontal Carpathians shortening, subsidence in the Focşani Basin and tilting of its western flank [*Gîrbacea and Frisch*, 1998]. However, the onset of Braşov basin sedimentation is lower Pliocene (upper Pontian), movements along the Carpathians sole thrust ended at 11 Ma (late Sarmatian) and tilting is Quaternary in age. A dense drip, of crustal or mantle type, has been proposed to migrate in time from the presently hot and lithospheric thin Pannonian basin toward the Carpathians slab [*Houseman and Gemmer*, 2005]. This migration must affect the upper crustal structure of the areas situated in between, such as the Transylvania basin, a rather stable

Figure 9. (a), (b) and (c) Conjugate normal faults observed at the surface in the neighborhood of an interpreted seismic line (Figure 9f, location "24,25"). One canyon with clear fault plane striations (Figure 9b) is associated with a step-like morphology and landsliding on the opposite fault plane (Figure 9c). (d) and (e) Large-scale landslides associated with the normal faults system, varying from kilometer size in the case of faults with larger (tens of meters) offsets (Figure 9d) to hundreds of meters in the case of smaller displacements in the order of meters or below (Figure 9e). The associated faults are visible in interpreted seismic profiles (Figure 9f, location "22,96"). (f) Interpreted seismic line along the NE flank of the Focşani basin; NTF, New Trotus Fault. Locations of seismic line and outcrops are given in Figure 7.

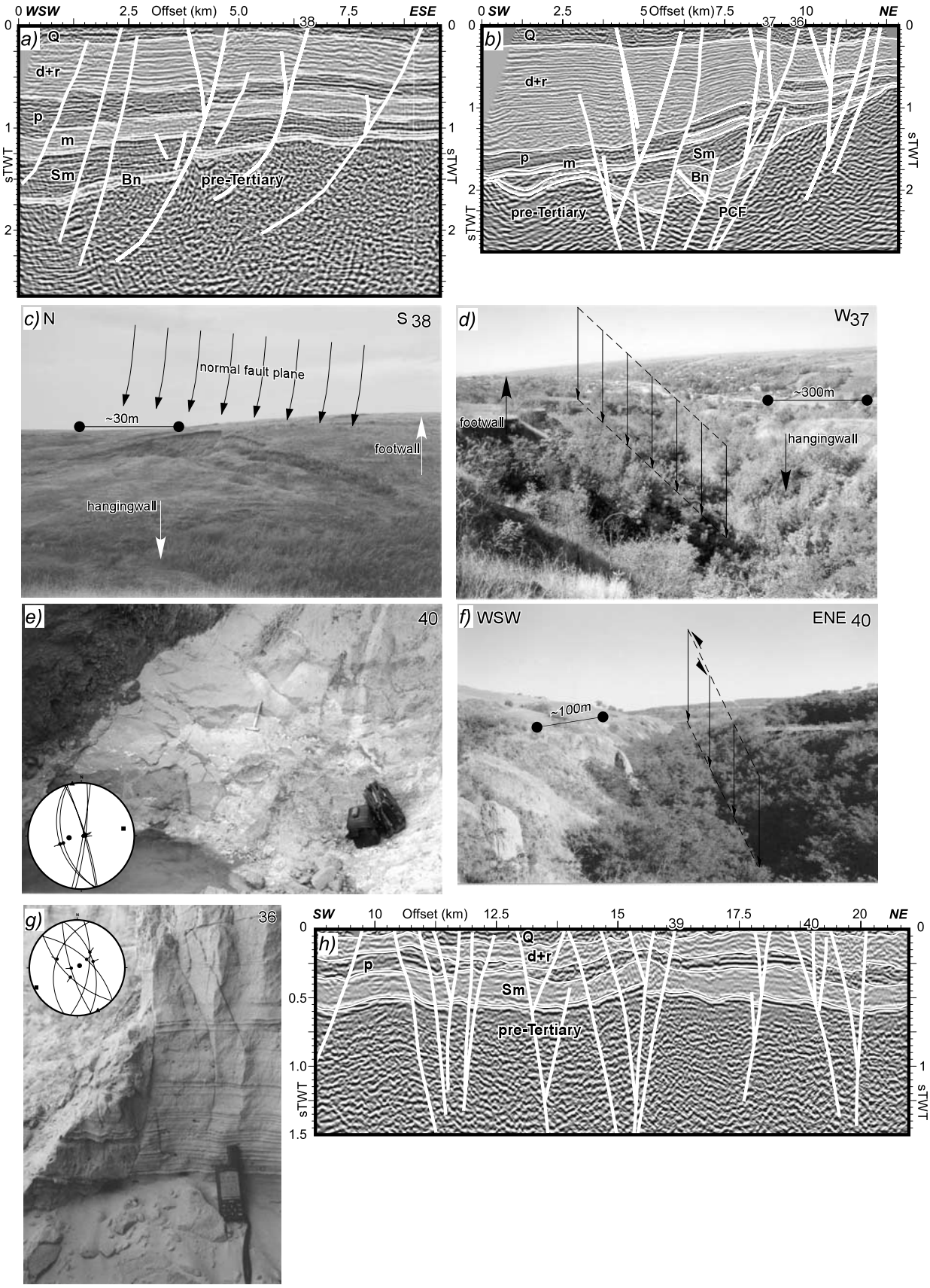
a)
WSW
Offset (km)
ESE
Q
d+r
p
m
Sm
Bn
pre-Tertiary
sTWT
b)
SW
Offset (km)
NE
Q
d+r
p
m
Sm
Bn
pre-Tertiary
PCF
sTWT
c)
N
S
38
normal fault plane
~30m
footwall
hangingwall
d)
W
37
~300m
footwall
hangingwall
e)
40
f)
WSW
ENE
40
~100m
g)
36
h)
SW
Offset (km)
NE
39
40
Q
d+r
p
Sm
pre-Tertiary
sTWT

Figure 10

block since its uplift ending at 9 Ma [*Krézsek and Bally*, 2006] with thick and cold lithosphere [*Demetrescu et al.*, 2001; *Dérerová et al.*, 2006].

[63] Slab detachment/break-off was active at the entire Carpathians scale [*Wortel and Spakman*, 2000], possibly during shortening and collision. Its continuation after 11 Ma would result in generalized uplift and not in the couple uplift/subsidence we observed at the scale of the East Carpathians. For further discussion on lateral migrating mechanisms at lithospheric scale and their impact on shallow vertical movements we refer to *Bertotti et al.* [2003].

5.1. Intraplate Folding

[64] One mechanism compatible with the observed uplift/subsidence couple is intraplate folding [e.g., *Cloetingh and Burov*, 1996] of a subducted system locked in early stages of Carpathians collision [*Cloetingh et al.*, 2004]. This couple is observed in the Pannonian area due to the Pliocene-Quaternary inversion [e.g., *Horváth and Cloetingh*, 1996; *Fodor et al.*, 2005] and is compatible with the Quaternary contraction observed in the SE Carpathians. In terms of folding wavelengths [e.g., *Cloetingh et al.*, 1999], the East European, Scythian and North Dobrogea foreland domain has an old thermotectonic age and therefore coupled crust and mantle, i.e., a lithospheric wavelength larger than the scale of the East Carpathians foreland. Uplift takes place here coevally along the coupled orogen-foreland system and with a similar impact on the present-day topography (Figure 12b). In contrast, Moesia must have a much shorter crustal wavelength due to recent, Miocene reheating events. Quaternary folding recorded comparable amounts of uplift in the orogen and subsidence in the foreland (Figure 12b).

[65] This model explains the Quaternary normal faulting which is observed near the contact between North Dobrogea orogen and Moesia as a mechanical contrast between their folding patterns. The former has an old, Cimmerian thermotectonic age [*Seghedi*, 2001], thus having a similar lithospheric uplift tendency in the foreland of the East Carpathians as neighboring East European and Scythian domains (Figure 12b). The contact with the subsiding basement of the Focşani syncline has reactivated the pre-Neogene Peceneaga-Camena fault as a wide zone of normal faulting (Figure 2). The fault is oblique to both the strike of the orogen and the axis of folding, which explains the lateral variability of deformation observed in the field. The Vrancea earthquakes have a curious spatial relationship with this fault, being located in its depth prolongation and these are recorded along the strike of the orogen as long as the fault exists, i.e., the mechanical contrast between North Dobrogea and Moesia (Figure 13).

5.2. Slab-Pull Versus Intraplate Shortening in the Aftermath of Collision

[66] All lithospheric mechanisms invoked for the SE Carpathians have one common element, the downward force (slab-pull) exerted by the >70 Ma old, thermally reequilibrating slab [e.g., *Cloetingh et al.*, 2004] visible on tomography studies [e.g., *Martin et al.*, 2006]. This process is coupled with the intraplate shortening generated by the (Pliocene) Quaternary inversion acting in the entire upper Carpathians plate as a response to Adria indentation (Figure 1c) [see *Bada et al.*, 1999]. Neither of these two mechanisms can self-explain the postcollisional patterns of the Romanian Carpathians.

[67] The latest Miocene–Pliocene subsidence was driven by slab-pull, as no coherent extensional phase can be defined to explain the observed subsidence. There is a clear spatial correlation between the position of the sediments depocenters in the Focşani basin, Vrancea seismicity and the main high-velocity body depicted by the seismic tomography (Figure 13). The surface affected by the slab-pull is confined to the area of the Moesian platform. The small zone between the pre-Neogene Trotus and New Trotus faults undergoing subsidence in the Scythian domain (Figure 2) is a drag fold at its contact with Moesia, subsequently faulted during the Quaternary (Figure 5c). Therefore the pulling part of the slab was attached only to Moesia and disconnected from the northern foreland blocks (Scythia/East Europe).

[68] The Quaternary contraction was driven by an overall intraplate shortening. Similar contractional patterns have been described in all westward units, such as Transylvania [e.g., *Ciulavu et al.*, 2000] and Pannonian basins [e.g., *Fodor et al.*, 2005], following the present-day stress trajectories in the upper Carpathians plate [e.g., *Bada et al.*, 1999; *Jarosinski et al.*, 2006]. induced by the counterclockwise rotation and northward indentation of the Adriatic microplate [e.g., *Grenerczy et al.*, 2005; *Pinter et al.*, 2005, and references therein]. These stress patterns are scattered to almost no preferential direction at the crustal scale of the SE Carpathians as observed in the World Stress Map data (B. Sperner, personal communication, 2007), probably as a result of local redistributions along particular structures on

Figure 10. (a)–(d) Depth and surface expression of the active fault system in the SE flank of the Focşani basin, often reactivating Sarmatian normal faults. Note the decreased width of the system and higher offsets in the seismic lines compared with Figures 8 and 9. Figures 10a and 10b show interpreted seismic lines across the pre-Neogene Peceneaga-Camena fault system (PCF). Note the reactivation of earlier normal faults during the Pliocene-Quaternary with clear offsets, roll-over anticlines, and massive seismic facies near the fault traces. Note also the thick wedge geometry of Pliocene strata. Figures 10c and 10d show outcrop-scale expression of the offset along the normal faults, either as small landslides (Figure 10c) or as canyons (Figure 10d). (e) and (f) Outcrop-scale expression of transcurrent movements detected in (g) interpreted seismic lines in the SE-most corner of the studied area. Centimeter-scale offsets in the Pliocene clastics (Figure 10e) are exaggerated to tens of meters deep canyons in the overlying loess deposits (Figure 10f). (h) Seismic line crossing the above described outcrops. Locations of seismic lines and outcrops are given in Figure 7.

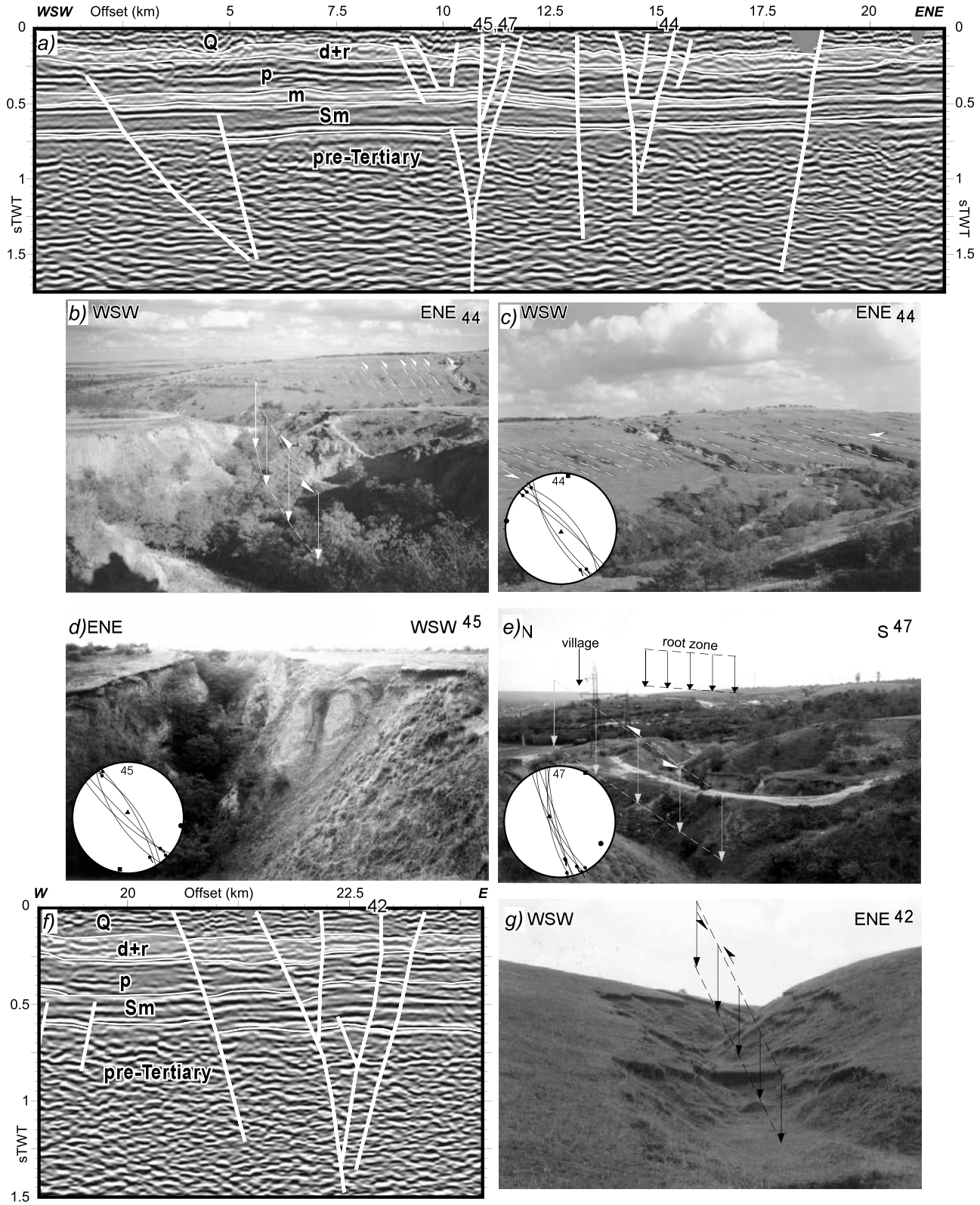
WSW
Offset (km)
5
7.5
10
12.5
15
17.5
20
ENE
45,47
44
a)
Q
d+r
p
m
Sm
pre-Tertiary
sTWT
b) WSW
ENE 44
c) WSW
ENE 44
d) ENE
WSW 45
e) N
S 47
village
root zone
W
20
Offset (km)
22.5
E
42
f)
g) WSW
ENE 42

Figure 11

the overall sinking pull given by the Vrancea slab [e.g., *Ismail-Zadeh et al.*, 2005]. Magnetic anisotropy results (AMS) recorded on sediments as young as the upper Pliocene were still able to record coherent strain patterns along the SE Carpathians structural grain [*Vasiliev*, 2006], possible driven by large values of intraplate stresses [*Tanasescu et al.*, 2005].

[69] The Carpathians stress trajectories are compatible with the WNW–ESE contraction observed in the Focşani basin (Figure 1c). Its onset is Pliocene in the Pannonian basin and the beginning of Quaternary in the SE Carpathians. The vertical movements 1 order of magnitude higher in the latter enable the speculation that Adria push is best felt in the Pannonian-Carpathians system at ~500 km away from the plates contact, in the Focşani basin. Lithospheric-scale asymmetries, such as the ones beneath the SE Carpathians, can represent stress and strain concentrations transmitted far away from the driving plate boundary.

[70] The uplift/exposure of the western Focşani flank was caused by a ~20 km shift of the null point and folding axial plane toward the foreland during the late Pleistocene (Figure 12a). This could have been caused by an increase in dip of the thermally reequilibrating slab at deep mantle levels which moved the slab, i.e., the lithospheric anisotropy, toward the foreland. This cannot be associated with a possible continuation of the slab retreat mechanism [e.g., *Royden*, 1988], because the orogenic contact with the foreland remains locked.

6. Active Tectonics

[71] Crustal seismicity in the SE Carpathians is more dispersed over the entire area between Trotus fault and Intramoesian fault than the intermediate-depth earthquakes (Figure 3). The crustal focal mechanisms do not indicate a consistent stress regime (Figures 3 and 13). These crustal events were generated by variable types of structures involving different kinematics (Figure 13). Although there is a large variability and further research is needed, we speculate that the normal faulting on the eastern and southern Focşani flank coincides with extensional solutions, compressional ones are a result of thick-skinned thrusting below the nappe pile, while the strike-slip solutions are preferably observed toward the boundaries of the folding area (compare Figures 3 and 13). Although is impossible to compute a particular generalized stress field on the basis of individual presently active structures nor from crustal focal mechanisms, the overall geometry of active deformation mechanism is characterized by folding in a WNW–ESE oriented corridor comprised between the Intramoesian and Trotus faults.

[72] Continuity of Quaternary deformation mechanisms until the present-day is in agreement with the preliminary GPS interpretations in terms of vertical motions (areas in uplift/subsidence) [*van der Hoeven et al.*, 2005]. Horizontal deformation takes place along the same boundaries (New Trotus, Peceneaga-Camena and Intramoesian faults). In terms of absolute rates of movements, 1.5 mm yr^{-1} of Quaternary subsidence is comparable with the 2–4 mm yr^{-1} GPS value in the Focşani basin. 1–2 mm yr^{-1} of GPS-measured uplift of the external nappes are somewhat less than the 4 mm yr^{-1} estimated by isotope geochronology studies [*Sanders et al.*, 1999]. This is most probably caused by a decrease in the uplift rates in the late Pleistocene–Holocene, as indicated by the <1 mm yr^{-1} derived from geomorphological reconstructions [*Necea et al.*, 2005].

[73] In terms of societal impact, the mantle seismicity, with a recurrence interval of 10 years for earthquakes with $M_w > 6.5$, 25 years for $M_w > 7$, and 50 years for $M_w > 7.5$ [*Oncescu and Trifu*, 1987] has a significant impact on largely populated areas [*Sokolov et al.*, 2004]. The collapse of the middle Pleistocene loess in the North Dobrogean unit is initiated by the movements of its underlying basement along active fault systems. This creates linear alignments of landslides in the SE Romanian Moldavia, frequently threatening densely populated areas (Figure 11e).

[74] Because of the active uplift/subsidence couple, the river network has an uncompensated character. The subsidence axis is used by the drainage collector of the East Carpathians, the Siret river, which actively deposits by meandering shifts and flooding in the Focşani basin, i.e., an area close to sea level (minimum 2.5 m above sea level, Figure 3). Active subsidence increases disequilibrium of the system and associated natural risk, as observed in recent years through larger flooding damages in the Focşani area (e.g., ~1.5 billion Euros worth of direct damages in 2005).

7. Conclusions

[75] The proposed Quaternary folding is based on the coexistence of apparently contrasting styles of deformation and associated vertical movements in a relatively restricted area of SE Carpathians. Reverse faults truncate the lower plate basement and the overlying thin-skinned units and are coeval with normal faulting in the distal parts of the foreland lacking a coherent direction of extension (Figures 1a and 2). This is contemporaneous with sinistral and dextral strike-slip movements along the northern and southern boundaries of the system, respectively (Figure 1a), as well as with out-

Figure 11. Large-scale transcurrent movements linked with the sinistral activity of the New Trotus Fault. Faults grouped in flower structures, visible in the interpreted seismic lines (Figures 11a and 11f), generate a large-scale collapse of surface topography. This is either visible through a dense network of en echelon structures, oblique to the trace of the valleys (Figures 11b and 11c), through deep canyons in loess with clear kinematics in the underlying Pliocene clastics (Figures 11b and 11d), or through large-scale landslides (Figure 11e). All types of canyons can be observed in the field, from initiation (Figures 11c and 11g) to mature, deep canyons (Figures 11b and 11d). For location of seismic lines and outcrops see Figure 7.

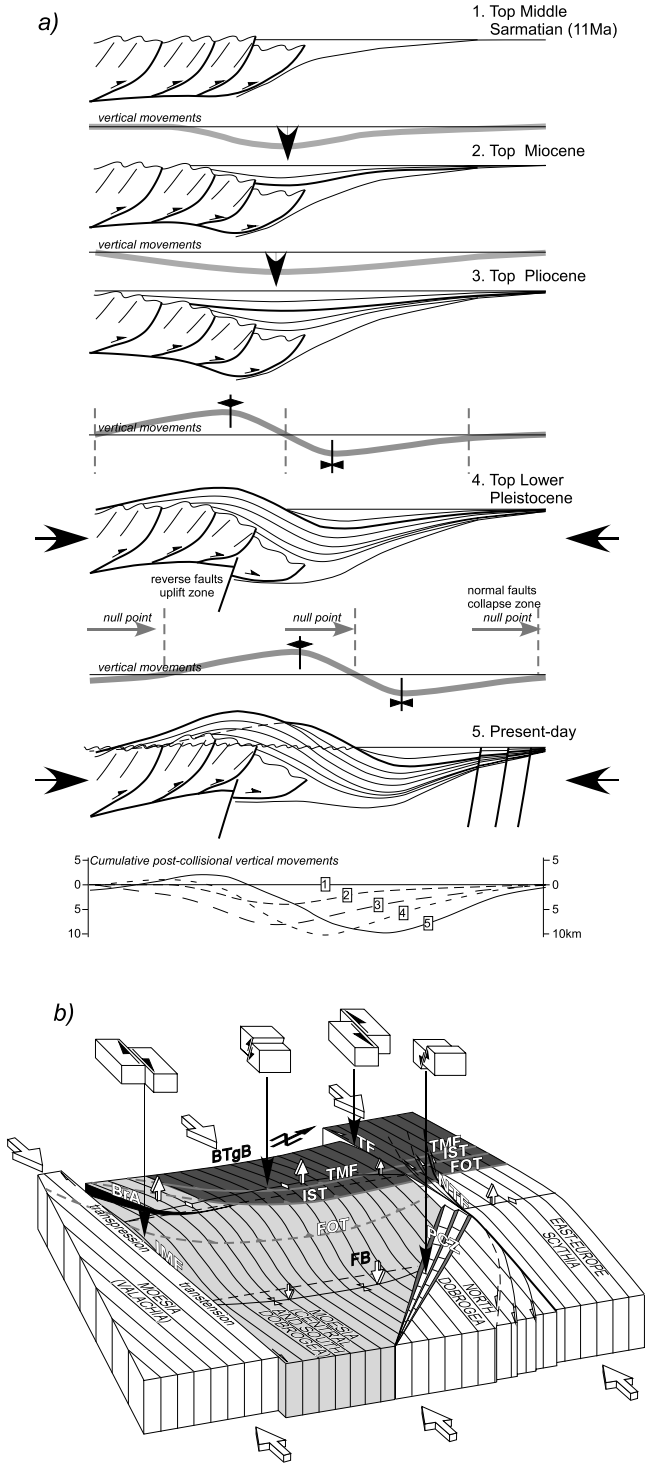

of-sequence oblique "Wallachian" thrusting (Figure 2). Vertical movements involve <5 km uplift of the external nappes and <2 km subsidence in the foreland. This deformation involves a total amount of <5 km WNW–ESE oriented shortening in a crust overlying the high-velocity mantle bodies (Vrancea slab and its pull) and intense seismicity (Figure 13). These features demonstrate that no coherent present-day regional stress field can or should be inferred on the basis of local observations. All the available information needs to be integrated for deriving a coherent tectonic scenario.

[76] Typically, along the Carpathians sector where the Moesian platform represents the foreland, the frontal part of the thin-skinned nappe pile is covered by postcollisional uppermost Miocene to Quaternary deposits with up to 5 km thickness. The particularly large subsidence in the center, i.e., the Focşani basin, associated with tilting on its western flank results its juxtaposition with a Quaternary age crustal folding mechanism acting in a restricted sector of the chain, between Intramoesian and (New) Trotus faults (Figures 1b and 12a). The associated vertical and horizontal movements have actively changed the shape of the basin, the overlying topography as well as the river network. The Quaternary deformation is presently active, and bears a significant human impact; besides the well studies Vrancea earthquakes, landslides and flooding represent two less known phenomena with comparable effects in the area.

Figure 12. (a) Cartoon illustrating the postcollisional evolution of the SE Carpathians and cumulative postorogenic movements. An initial phase of subsidence during the late Miocene and Pliocene was subsequently followed by folding during the Quaternary. Two folding phases are observed, with a migration of the null point (vertical movements zero) during the middle Pleistocene. The amplitude of vertical cumulative postcollisional movements and the amount of null point migration are rough values from isotope geochronology, basin, and geomorphology studies (see description in text for further details). Note the large differences in the particle tracking during the postcollisional vertical movements between the external nappes and the foreland. (b) Illustration of the folding effects at two different wavelengths in the foreland of the East Carpathians, as a function of the differences in rheology of the lower plate. While the entire East European/Scythian/North Dobrogea domain is under uplift, Moesia displays folding at shorter wavelength. At the transition between the two domains, sinistral strike-slip movement concentrates along the New Trotus Fault, while normal faults follow the Peceneaga-Camena fault. Note that these faults act as transfer/tear faults during the Quaternary shortening; their upthrown or downthrown components are purely the result of folding. FOT, frontal orogenic thrust; IST, intra-Subcarpathian thrust; TMF, Tarcau/Marginal Folds thrust front; (N)TF, (New) Trotus Fault; IMF, Intramoesian fault; PCZ, Peceneaga-Camena fault zone (including Siret fault); BrA, Breaza anticline thrust; BTgB, Braşov and Tîrgu Secuiesc basins; FB, Focşani basin.

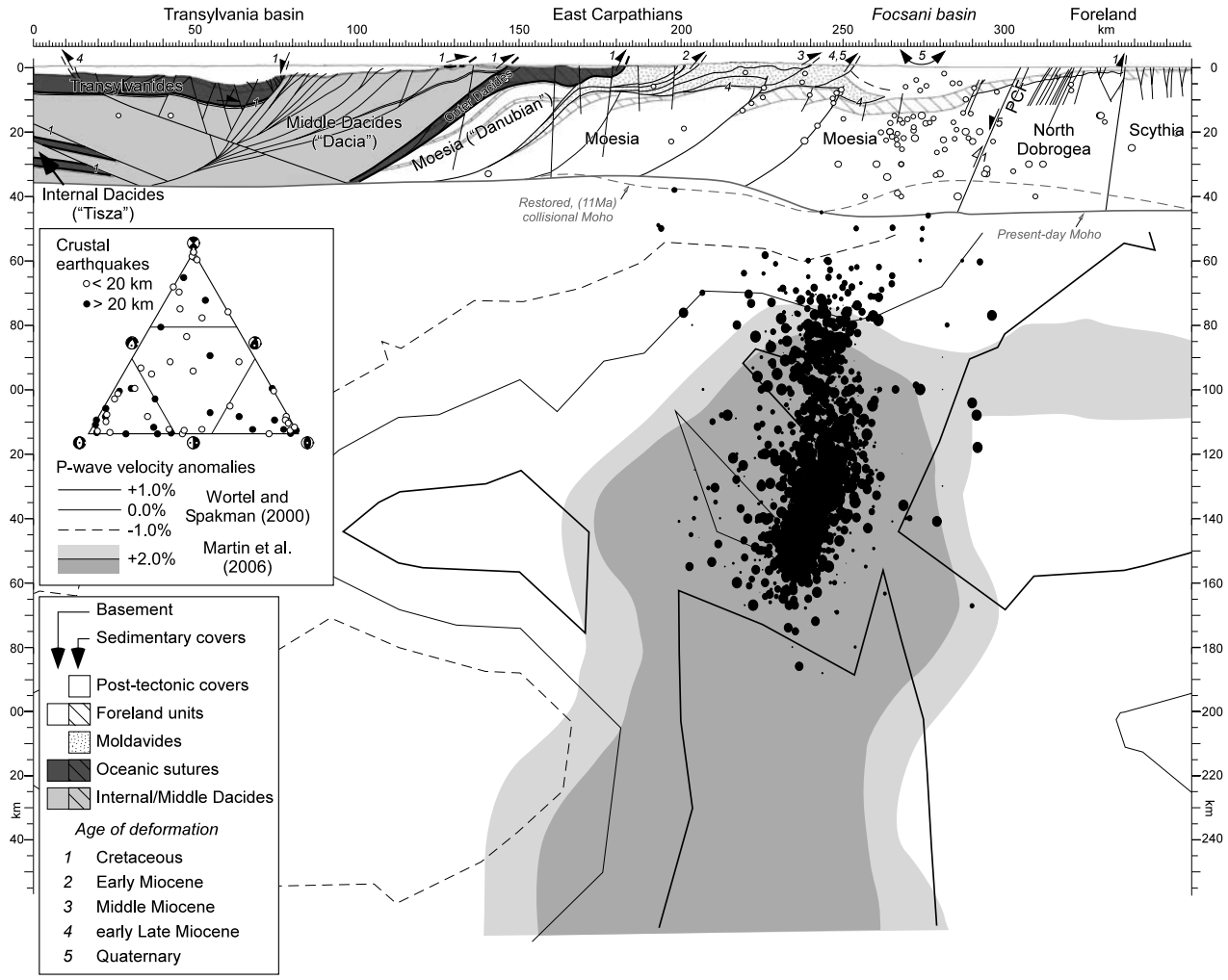

Figure 13. Simplified tectonic cross section across the Romanian Carpathians. See *Schmid et al.* [2007] for further details. Interpretation of faults in the lower crust (>20 km) is speculative. PCF, Pecenaga-Camena Fault. Present-day Moho surface and the geometry of PCF are after *Radulescu et al.* [1976] and *Hauser et al.* [2007]. The Moho surface is reconstructed for the moment of collision (~11 Ma, gray dashed line), retrodeforming subsequent cumulative postcollisional vertical movements, as indicated in Figure 12a. Earthquakes from the SE Carpathians were projected into the cross section as a function of depth and magnitude. Crustal seismicity was projected perpendicular to the cross section (i.e., along the strike of the Quaternary folding), while mantle earthquakes were projected along the strike of the NE-SW oriented intermediate Vrancea mantle slab, oblique to the trace of the cross section (see Figure 3). The ternary diagram represents the types of focal mechanisms for the crustal earthquakes. P wave velocity anomalies are after the regional seismic tomography of *Wortel and Spakman* [2000] and *Martin et al.* [2006]. Note that only positive anomalies with a rough position at depth are displayed for the latter. For complete a section at the regional Carpathians scale, see *Wortel and Spakman* [2000] and *Martin et al.* [2006].

[77] The two deformation episodes proposed, latest Miocene–Pliocene subsidence and Quaternary folding, represent an effect of the interplay between two mechanisms, the pull-down effect of a slab inherited and locked during the late Miocene collision and the Quaternary inversion of the entire Carpathians-Pannonian system.

[78] Our data concentrate on the shallow part of the crust, often ignored or at odds with many Carpathians models focused at deep lithospheric levels. This data set demonstrates that integration of shallow geological and deep geophysical data is a prerequisite to derive the interaction and feedback mechanisms between lithospheric controls on (near)surface processes.

[79] **Acknowledgments.** This research forms part of the Pannonian-Carpathians programme of the Netherlands Centre for Integrated Solid Earth Science (ISES). The research was carried out in collaboration between Vrije University Amsterdam, University of Basel, and University of Bucharest. Most of the fieldwork studies and initial data processing have been funded by the Swiss National Science Foundation SCOPES project 7RUPJ062307.00/1. We acknowledge the Romanian National Agency of Mineral Resources, Forest Oil International, SNP Petrom SA, and Rompetrol SA for granting access to the depth data. Fruitful discussions and collaboration with R. Stephenson, G. Bada, M. Săndulescu, M. Marin, V. Diaconescu, M. Tilita, I. Panea, I. Vasiliev, C. Langereis, D. Necea, A. Bocin, M. Stoica, I. Seghedi, J.H. Knapp, and C.C. Knapp have substantially improved the quality of the manuscript. V. Raileanu is thanked for collaboration in analyzing the deep Vrancea mechanisms. M. Radulian is thanked for sharing the electronic version of the focal mechanism database published in 2002. Two anonymous reviewers are acknowledged for the unusual large amount of suggestions clear upgrading the initial manuscript. B. Sperner is thanked for the extensive review and useful suggestions.

References

Angelier, J. (1984), Tectonic analysis of fault slip data sets, *J. Geophys. Res.*, *89*, 5835–5848.

Angelier, J. (1989), From orientation to magnitudes in paleostress determination using fault slip data, *J. Struct. Geol.*, *11*, 37–50.

Bada, G., F. Horváth, P. Gerner, and I. Fejes (1999), Review of the present-day geodynamics of the Pannonian Basin; progress and problems, *J. Geodyn.*, *27*, 501–527.

Bada, G., F. Horváth, S. Cloetingh, D. D. Coblentz, and T. Tóth (2001), Role of topography-induced gravitational stresses in basin inversion: The case study of the Pannonian basin, *Tectonics*, *20*(3), 343–363.

Bâlă, A., M. Radulian, and E. Popescu (2003), Earthquakes distribution and their focal mechanism in correlation with the active tectonic zones of Romania, *J. Geodyn.*, *36*(1–2), 129–145, doi:10.1016/S0264-3707 (03)00044-9.

Balla, Z. (1986), Paleotectonic reconstruction of the central Alpine-Mediterranean belt for the Neogene, *Tectonophysics*, *127*, 213–243.

Batt, G. E., and J. Braun (1999), The tectonic evolution of the Southern Alps, New Zealand: Insights from fully thermally coupled dynamical modelling, *Geophys. J. Int.*, *136*, 403–420.

Beaumont, C. (1981), Foreland basins, *Geophys. J. R. Astron. Soc.*, *65*, 291–329.

Bertotti, G., V. Picotti, C. Chilovi, R. Fantoni, S. Merlini, and A. Mosconi (2001), Neogene to Quaternary sedimentary basins in the south Adriatic (central Mediterranean): Foredeeps and lithospheric buckling, *Tectonics*, *20*(5), 771–787.

Bertotti, G., L. Matenco, and S. Cloetingh (2003), Vertical movements in and around the SE Carpathian foredeep: Lithospheric memory and stress field control, *Terra Nova*, *15*, 299–305, doi:10.1046/j.1365-3121.2003.00499.x.

Bocin, A., R. Stephenson, A. Tryggvason, I. Panea, V. Mocanu, F. Hauser, and L. Matenco (2005), 2.5D seismic velocity modelling in the southeastern Romanian Carpathians Orogen and its foreland, *Tectonophysics*, *410*, 273–291, doi:10.1016/j.tecto.2005.05.045.

Ciulavu, D., C. Dinu, A. Szakacs, and D. Dordea (2000), Late Miocene to Pliocene kinematics of the Transylvania basin, *AAPG Bull.*, *84*, 1589–1615.

Clauzon, G., J.-P. Suc, S.-M. Popescu, M. Marunteanu, J.-L. Rubino, F. Marinescu, and M. C. Melinte (2005), Influence of Mediterranean sea-level changes on the Dacic Basin (Eastern Paratethys) during the late Neogene: The Mediterranean Lago-Mare facies deciphered, *Basin Res.*, *17*, 437–462, doi:10.1111/j.1365-2117.2005.00269.x.

Cloetingh, S., and E. B. Burov (1996), Thermomechanical structure of European continental lithosphere: Constraints from rheological profiles and EET estimates, *Geophys. J. Int.*, *124*, 695–723.

Cloetingh, S., E. Burov, and A. Poliakov (1999), Lithosphere folding: Primary response to compression? (from central Asia to Paris basin), *Tectonics*, *18*(6), 1064–1083.

Cloetingh, S., F. Horváth, C. Dinu, R. A. Stephenson, G. Bertotti, G. Bada, L. Matenco, and D. Garcia-Castellanos (2003), Probing tectonic topography in the aftermath of continental convergence in central Europe, *Eos Trans. AGU*, *84*(10), 89.

Cloetingh, S., E. Burov, L. Matenco, G. Toussaint, G. Bertotti, P. A. M. Andriessen, M. J. R. Wortel, and W. Spakman (2004), Thermo-mechanical controls on the mode of continental collision in the SE Carpathians (Romania), *Earth Planet. Sci. Lett.*, *218*(1–2), 57–76, doi:10.1016/S0012-821X (03)00645-9.

Csontos, L., and A. Vörös (2004), Mesozoic plate tectonic reconstruction of the Carpathian region, *Paleogeogr. Paleoclimatol. Paleoecol.*, *210*(1), 1–56, doi:10.1016/j.palaeo.2004.02.033.

Demetrescu, C., S. B. Nielsen, M. Enea, D. Z. Şerban, G. Polonic, M. Andreescu, A. Pop, and N. Balling (2001), Lithosphere thermal structure and evolution of the Transylvanian Depression—Insights from new geothermal measurements and modelling results, *Phys. Earth Planet. Inter.*, *126*, 249–267.

Dérerová, J., H. Zeyen, M. Bielik, and K. Salman (2006), Application of integrated geophysical modeling for determination of the continental lithospheric thermal structure in the eastern Carpathians, *Tectonics*, *25*, TC3009, doi:10.1029/2005TC001883.

Dewey, J. F. (1980), Episodicity, sequence and style at convergent plate boundaries, in *The Continental Crust and Its Mineral Deposits*, edited by D. W. Strangway, pp. 553–573, Geol. Assoc. of Can., Waterloo, Ontario.

Dicea, O. (1995), The structure and hydrocarbon geology of the Romanian East Carpathians border from seismic data, *Petrol. Geosci.*, *1*, 135–143.

Diehl, T., J. R. R. Ritter, and CALIXTO Working Group (2005), The crustal structure beneath SE Romania from teleseismic receiver functions, *Geophys. J. Int.*, *163*, 238–251, doi:10.1111/j.1365-246X. 2005.02715.x.

Ellouz, N., and E. Roca (1994), Palinspastic reconstructions of the Carpathians and adjacent areas since the Cretaceous: A quantitative approach, in *Peri-Tethyan Platforms*, edited by F. Roure, pp. 51–78, Technip, Paris.

Ellouz, N., F. Roure, M. Săndulescu, and D. Badescu (1994), Balanced cross sections in the eastern Carpathians (Romania): A tool to quantify Neogene dynamics, in *Geodynamic Evolution of Sedimentary Basins, International Symposium Moskow 1992 Proceedings*, edited by F. Roure et al., pp. 305–325, Technip, Paris.

Fielitz, W., and I. Seghedi (2005), Late Miocene–Quaternary volcanism, tectonics and drainage system evolution in the East Carpathians, Romania, *Tectonophyiscs*, *410*(1–4), 111–136, doi:10.1016/j.tecto.2004.10.018.

Fodor, L., G. Bada, G. Csillag, E. Horváth, Z. Ruszkiczay-Rudiger, K. Palotas, F. Sikhegyi, G. Timar, S. Cloetingh, and F. Horváth (2005), An outline of neotectonic structures and morphotectonics of the western and central Pannonian Basin, *Tectonophysics*, *410*, 15–41, doi:10.1016/j.tecto.2005.06.008.

Fügenschuh, B., and S. M. Schmid (2005), Age and significance of core complex formation in a very curved orogen: Evidence from fission track studies in the South Carpathians (Romania), *Tectonophyiscs*, *404*(1–2), 33–53, doi:10.1016/j.tecto.2005.03.019.

Garcia-Castellanos, D. (2002), Interplay between lithospheric flexure and river transport in foreland basins, *Basin Res.*, *14*, 89–104.

Ghenea, C., T. Brandabur, N. Mihăilă, A. Ghenea, and P. Giurgea (1971), România, Harta Cuaternarului, scale 1:1,000,000, Inst. Geol. al României, Bucharest.

Gillet, H., G. Lericolais, J.-P. Rehault, and C. Dinu (2003), La stratigraphie oligo-miocene et la surface d'érosion messinienne en mer Noire, stratigraphie sismique haute resolution, *C. R. Geosci.*, *335*, 907–916, doi:10.1016/j.crte.2003.08.008.

Gîrbacea, R., and W. Frisch (1998), Slab in the wrong place: Lower lithospheric mantle delamination in the last stage of the eastern Carpathians subduction retreat, *Geology*, *26*, 611–614.

Grenerczy, G., G. Sella, S. Stein, and A. Kenyeres (2005), Tectonic implications of the GPS velocity field in the northern Adriatic region, *Geophys. Res. Lett.*, *32*, L16311, doi:10.1029/2005GL022947.

Gusev, A., M. Radulian, M. Rizescu, and G. F. Panza (2002), Source scaling of intermediate-depth Vrancea earthquakes, *Geophys. J. Int.*, *151*, 879–889.

Gvirtzman, Z. (2002), Partial detachment of a lithospheric root under the southeast Carpathians: Toward a better definition of the detachment concept, *Geology*, *30*, 51–54.

Hauser, F., V. Raileanu, W. Fielitz, C. Dinu, M. Landes, A. Bala, and C. Prodehl (2007), Seismic crustal structure between the Transylvanian Basin and the Black Sea, Romania, *Tectonophysics*, *430*, 1–25, doi:10.1016/j.tecto.2006.10.005.

Hippolyte, J. C., and M. Săndulescu (1996), Paleostress characterization of the "Wallachian" phase in its type area, southeastern Carpathians, Romania, *Tectonophysics*, *263*, 235–249.

Horváth, F. (1993), Towards a mechanical model for the formation of the Pannonian basin, *Tectonophysics*, *226*, 333–357.

Horváth, F., and S. Cloetingh (1996), Stress-induced late-stage subsidence anomalies in the Pannonian basin, *Tectonophysics*, *266*, 287–300.

Houseman, G. A., and L. Gemmer (2005), Lithospheric extension within a continental orogen: The Pannonian Basin, *Eos Trans. AGU*, *86*(52), Fall Meet. Suppl., Abstract U51B-01.

Ismail-Zadeh, A., et al. (2005), Three-dimensional numerical modeling of contemporary mantle flow and tectonic stress beneath the earthquake-prone southeastern Carpathians based on integrated analysis of seismic, heat flow, and gravity data, *Phys. Earth Planet. Inter.*, *149*, 81–98.

Jarosinski, M., F. Beekman, G. Bada, and S. Cloetingh (2006), Redistribution of recent collision push and ridge push in Central Europe: Insights from FEM modelling, *Geophys. J. Int.*, *167*, 860–880.

Jipa, D. (1997), Late Neogene-Quaternary evolution of Dacian basin (Romania). An analysis of sediment thickness pattern, *Geo Eco Marina*, *2*, 128–134.

Knapp, J. H., C. C. Knapp, V. Raileanu, L. Matenco, V. Mocanu, and C. Dinu (2005), Crustal constraints on the origin of mantle seismicity in the Vrancea Zone, Romania: The case for active continental lithospheric delamination, *Tectonophysics*, *410*, 311–323, doi:10.1016/j.tecto.2005.02.020.

Krézsek, C., and A. Bally (2006), The Transylvanian Basin (Romania) and its relation to the Carpathian

fold and thrust belt: Insights in gravitational salt tectonics, *Mar. Pet. Geol.*, *23*, 405–442.

Landes, M., W. Fielitz, F. Hauser, and M. Popa (2004), 3-D upper crustal tomographic structure across the Vrancea seismic zone, Romania, *Tectonophysics*, *382*, 85–102, doi:10.1016/j.tecto.2003.11.013.

Lăzărescu, V., I. Cornea, F. Rădulescu, and M. Popescu (1983), Moho surface and Recent crustal movements in Romania: Geodynamic connections, *Annu. Inst. Geol. Geophys. Bucharest*, *63*, 83–91.

Leever, K., L. Matenco, G. Bertotti, S. Cloetingh, K. G. Drijkoningen, and I. Vasiliev (2006), Pliocene to Recent kinematics in the Focşani basin, Romania: New constraints from shallow seismic and paleomagnetic data, *Basin Res.*, *18*, 521–545, doi:10.1111/j.1365-2117.2006.00306.x.

Marinescu, F., and I. Papaianopol (1995), La Depression de Transylvanie; le basin Braşov-Baraolt, in *Chronostratigraphie und Neostratotypen, Pliozan Pl1, Dazien*, edited by F. Marinescu and I. Papaianopol, pp. 82–83, Acad. Romane, Bucharest.

Martin, M., F. Wenzel, and CALIXTO Working Group (2006), High-resolution teleseismic body wave tomography beneath SE Romania: II. Imaging of a slab detachment scenario, *Geophys. J. Int.*, *164*, 579–595, doi:10.1111/j.1365-246X.2006.02884.x.

Mărunţeanu, M., and L. Papaianopol (1995), The connection between the Dacic and Medirranean basins based on calcareous nannoplankton assemblages, *Rom. J. Stratigr.*, *76*, 169–170.

Matenco, L., and G. Bertotti (2000), Tertiary tectonic evolution of the external East Carpathians (Romania), *Tectonophysics*, *316*, 255–286.

Matenco, L., and S. Schmid (1999), Exhumation of the Danubian nappes system (South Carpathians) during the early Tertiary: Inferences from kinematic and paleostress analysis at the Getic/Danubian nappes contact, *Tectonophysics*, *314*, 401–422.

Matenco, L., G. Bertotti, S. Cloetingh, and C. Dinu (2003), Subsidence analysis and tectonic evolution of the external Carpathian-Moesian platform region during Tertiary times, *Sediment. Geol.*, *156*, 71–94.

Merten, S., P. A. M. Andriessen, J. Juez-Larré, G. Bertotti, and T. J. Dunai (2005), Dating the exhumation of the Romanian Carpathians: First results from apatite (U-Th)/He thermochronology, *Geophys. Res. Abs.*, *7*, 08138.

Morley, C. K. (1996), Models for relative motion of crustal blocks within the Carpathian region, based on restorations of the outer Carpathian thrust sheets, *Tectonics*, *15*(4), 885–904, doi:10.1029/95TC03681.

Necea, D., W. Fielitz, and L. Matenco (2005), Late Pliocene-Quaternary large scale differential motions in the frontal part of the SE Carpathians: Insights from tectonic geomorphology, *Tectonophyiscs*, *410*, 137–156.

Olteanu, R. (2003), The last representatives of ''the Pannonian'' realm (Ostracoda, Crustacea), in *Chronostratigraphie und Neostratotypen, Pliozan Pl2, Romanien*, edited by I. Papaianopol, F. Marinescu, N. Krstic, and R. Macalalet, pp. 350–375, Acad. Romane, Bucharest.

Oncescu, M. C. (1984), Deep structure of the Vrancea region, Romania, inferred from simultaneous inversion for hypocenters and 3-D velocity structure, *Ann. Geophys.*, *2*, 23–28.

Oncescu, M. C., and K. P. Bonjer (1997), A note on the depth recurrence and strain release of large Vrancea earthquakes, *Tectonophysics*, *272*, 291–302.

Oncescu, M. C., and C. I. Trifu (1987), Depth variation of the moment tensor principal axes in Vrancea (Romania) seismic region, *Ann. Geophys.*, *5B*, 149–154.

Papaianopol, I., D. Jipa, F. Marinescu, N. Ticleanu, and R. Macalalet (1995), Upper Neogene from the Dacian basin, *Romanian J. Stratigr.*, *76*, 33–43.

Pharaoh, T. C. (1999), Palaeozoic terranes and their lithospheric boundaries within the Trans-European Suture Zone (TESZ): A review, *Tectonophysics*, *314*, 17–41.

Pinter, N., G. Grenerczy, J. Weber, S. Stein, and D. Medak (2005), *The Adria Microplate: GPS Geodesy, Tectonics and Hazards*, *NATO Sci. Ser. IV, Earth and Environmental Sciences*, 413 pp., Springer, New York.

Popescu, M. N., and I. Dragoescu (1986), The new map of recent vertical crustal movements in Romania, scale 1:1,000,000, *Rev. Roum. Geol. Geophys. Geogr., Ser. Geophys.*, *30*, 10–31.

Posea, G. (1981), The Braşov Depression: Geomorphologic characteristics, *An. Univ. Bucuresti, Ser. Geogr.*, *30*, 19–38.

Prosser, S. (1993), Rift related depositional system and their seismic expression, in *Tectonics and Seismic Sequence Stratigraphy*, edited by G. D. Williams and A. Dobb, *Geol. Soc. Spec. Publ.*, *71*, 35–66.

Răbăgia, T., and L. Matenco (1999), Tertiary tectonic and sedimentological evolution of the South Carpathians foredeep: Tectonic versus eustatic control, *Mar. Pet. Geol.*, *16*, 719–740.

Răbăgia, T., and M. Tărăpoancă (1999), Tectonic evolution of the Romanian part of the Moesian platform: An integrated model, *Romanian J. Tectonics Reg. Geol.*, *77*, 58.

Rabus, B., M. Eineder, A. Roth, and R. Bamler (2003), The shuttle radar topography mission—New class of digital elevation models acquired by spaceborne radar, *Photogram. Remote Sens.*, *57*, 241–262.

Rădoane, M., N. Rădoane, and D. Dumitriu (2003), Geomorphological evolution of longitudinal river profiles in the Carpathians, *Geomorphology*, *50*(4), 293–306, doi:10.1016/S0169-555X (02)00194-0.

Radulescu, D. P., et al. (1976), Structure de la côute terrestre en Roumanie. Essai d'interprétation des études séismiques profondes, *An. Inst. Geol. Geofiz.*, *50*, 5–36.

Rădulescu, F. (1988), Seismic models of the crustal structure in Romania, *Rev. Roum. Geol. Geophys. Geogr., Ser. Geophys.*, *32*, 13–17.

Radulian, M., N. Mandrescu, G. F. Panza, E. Popescu, and A. Utale (2000), Characterization of seismogenic zones of Romania, in *Seismic hazards of the Circum-Pannonian region*, *Pure and Applied Geophysics*, edited by Panza et al., pp 55–77, Birkhaeuser, Basel, Switzerland.

Radulian, M., E. Popescu, A. Bâlă, and A. Utale (2002), Catalog of fault plane solutions for the earthquakes occurred on the Romanian territory, *Romanian J. Phys.*, *47*, 663–685.

Rögl, F. (1996), Stratigraphic correlation of Paratethys Oligocene and Miocene, *Mitt. Ges. Geol. Bergbaustud. Oesterr.*, *41*, 65–73.

Roure, F., E. Roca, and W. Sassi (1993), The Neogene evolution of the outer Carpathian flysch units (Poland, Ukraine and Romania): Kinematics of a foreland/fold-and-thrust belt system, *Sediment. Geol.*, *86*, 177–201.

Royden, L. (1988), Flexural behavior of the continental lithosphere in Italy: Constraints imposed by gravity and deflection data, *J. Geophys. Res.*, *93*, 7747–7766.

Royden, L. H. (1993), Evolution of retreating subduction boundaries formed during continental collision, *Tectonics*, *12*, 629–638.

Sacks, P. E., and D. T. Secor (1990), Delamination in collisional orogens, *Geology*, *18*, 999–1002.

Sanders, C. A. E., P. A. M. Andriessen, and S. A. P. L. Cloetingh (1999), Life cycle of the East Carpathian orogen: Erosion history of a doubly vergent critical wedge assessed by fission track thermochronology, *J. Geophys. Res.*, *104*, 29,095–29,112.

Săndulescu, M. (1980), Analyse géotectonique des chaînes alpines situées autour de la Mer Noire occidentale, *Ann. Inst. Geol. Geophys.*, *56*, 5–54.

Săndulescu, M. (1984), *Geotectonica României* (*Geotectonics of Romania*), 450 pp, Tehnicã, Bucharest.

Săndulescu, M. (1988), Cenozoic Tectonic History of the Carpathians, in *The Pannonian Basin, a Study in Basin Evolution*, edited by L. H. Royden and F. Horváth, *AAPG Mem.*, 45, 17–25.

Săndulescu, M., and M. Visarion (1977), Considerations sur la structure tectonique du soubassement de la depression de Transilvanie, *Dari Seama Sedintelor*, *64*, 153–173.

Săndulescu, M., and M. Visarion (1988), La structure des plate-formes situées dans l'avant-pays et au-dessous des nappes du flysch des Carpathes orientales, *St. Tehn. Econ. Geofiz.*, *15*, 62–67.

Schmid, S. M., T. Berza, V. Diaconescu, N. Froitzheim, and B. Fuegenschuh (1998), Orogen-parallel extension in the South Carpathians during the Paleogene, *Tectonophysics*, *297*, 209–228.

Schmid, S. M., B. Fugenschuh, L. Matenco, R. Schuster, M. Tischler, and K. Ustaszewski (2007), The Alps-Carpathians-Dinarides-connection: A compilation of tectonic units, *Eclogae Geol. Helv.*, in press.

Seghedi, A. (2001), The North Dobrogea orogenic belt (Romania); a review, in *Peri-Tethys Memoir 6; Peri-Tethyan Rift/Wrench Basins and Passive Margins*, edited by P. A. Ziegler et al., *Mem. Mus. Natl. Hist. Nat.*, *186*, 237–257.

Sokolov, V., K.-P. Bonjer, and F. Wenzel (2004), Accounting for site effect in probabilistic assessment of seismic hazard for Romania and Bucharest: A case of deep seismicity in Vrancea zone, *Soil Dyn. Earthquake Eng.*, *24*(12), 929–947, doi:10.1016/j.soildyn.2004.06.021.

Ştefănescu, M., et al. (1988), Geological cross sections at scale 1:200,000, *Map A9–14*, Inst. Geol. Geofiz., Bucharest.

Ştefănescu, M., O. Dicea, G. Tari (2000), Influence of extension and compression on salt diapirism in its type area, East Carpathians Bend area, Romania, in *Salt, Shale and Igneous Diapirs in and Around Europe*, edited by B. C. Vendeville, Y. Mart, and J. L. Vigneresse, *Geol. Soc. Spec. Publ.*, *174*, 131–147.

Tanasescu, G., W. Spakman, and B. A. C. Ambrosius (2005), Surface deformation of the Vrancea region (Romania) from inversion of GPS motion vectors, *Geophys. Res. Abstr.*, *7*, 07317.

Tărăpoancă, M., G. Bertotti, L. Matenco, C. Dinu, and S. Cloetingh (2003), Architecture of the Focşani depression: A 13 km deep basin in the Carpathians bend zone (Romania), *Tectonics*, *22*(6), 1074, doi:10.1029/2002TC001486.

Tărăpoancă, M., D. Garcia-Castellanos, G. Bertotti, L. Matenco, S. Cloetingh, and C. Dinu (2004), Role of the 3D distributions of load and lithospheric strength in orogenic arcs: Poly-stage subsidence in the Carpathians foredeep, *Earth Planet. Sci. Lett.*, *221*(1–4), 163–180, doi:10.1016/S0012-821X(04)00068-8.

Toussaint, G., E. Burov, and L. Jolivet (2004), Continental plate collision: Unstable vs. stable dynamics, *Geology*, *32*(1), 33–36, doi:10.1130/G19883.1.

Toutin, T. (2002), Three-dimensional topographic mapping with ASTER stereo data in rugged topography, *Trans. Geosci. Remote Sens.*, *40*, 2241–2247.

Vaida, M., A. Seghedi, and J. Verniers (2005), Northern Gondwanan affinity of the East Moesian Terrane based on chitinozoans, *Tectonophyiscs*, *410*, 379–387, doi:10.1016/j.tecto.2004.12.039.

van der Hoeven, A. G. A., V. Mocanu, W. Spakman, M. Nutto, L. Nuckelt, L. Matenco, L. Munteanu, C. Marcu, and B. A. C. Ambrosius (2005), Observation of Present-day tectonic motions in the south-eastern Carpathians: Geodetic results of the ISES/CRC-461 GPS measurements, *Earth Planet. Sci. Lett*, *239*(3–4), 177–184, doi:10.1016/j.epsl.2005.09.018.

Vasiliev, I. (2006), A new chronology for the Dacian basin (Romania): Consequences for the kinematic and paleoenvironmental evolution of the Paratethys region, Ph.D. thesis, 193 pp., Univ. Utrecht, Utrecht.

Vasiliev, I., W. Krijgsman, C. G. Langereis, C. E. Panaiotu, L. Matenco, and G. Bertotti (2004), Magnetostratigraphyc dating and astronomical forcing of the Mio-Pliocene sedimentary sequences of the Focşani basin (eastern Paratethys-Romania), *Earth Planet. Sci. Lett*, *227*(1–2), 231–247, doi:10.1016/j.epsl.2004.09.012.

Vermeersen, L. L. A., J. van Hove, A. G. A. van der Hoeven, and R. E. M. Riva (2004), Post-seismic deformation in the Vrancea region, Romania, *Geophys. Res. Abstr.*, *6*, 01888.

Visarion, C. M., and R. Rotaru (1988), Contributii geoelectrice la studiul subasmentului cretacic al Depresiunii Birsei, *St. Tehn. Econ. Geofiz.*, *15*, 203–210.

Visarion, M., M. Săndulescu, D. Stănică, and L. Atanasiu (1988a), An improved geotectonic model of the East Carpathians, *Rev. Roumania Geol. Geophys et Geogr., Ser. Geophys.*, *32*, 43–52.

Visarion, M., M. Săndulescu, D. Stănică, and S. Veliciu (1988b), Contributions à la connaissance de la structure profonde de la plate-forme Moésienne en Roumanie, *St. Tehn. Econ. Geofiz.*, *15*, 68–92.

Weidle, C., S. Widiyantoro, and CALIXTO Working Group (2005), Improving depth resolution of teleseismic tomography by simultaneous inversion of teleseismic and global P-wave traveltime data: Application to the Vrancea region in southeastern Europe, *Geophys. J. Int.*, *162*, 811–823, doi:10.1111/j.1365-246X.2005.02649.x.

Wenzel, F., F. Lorenz, B. Sperner, and M. C. Oncescu (1999), Seismotectonics of the Romanian Vrancea area, in *Vrancea Earthquakes: Tectonics, Hazard and Risk Mitigation*, edited by F. Wenzel, D. Lungu, and O. Novak., pp. 15–26, Kluwer Acad., Dordrecht, Netherlands.

Williams, G. D., C. M. Powell, and M. A. Cooper (1989), Geometry and kinematics of inversion tectonics, in *Inversion Tectonics*, edited by M. A. Cooper and G. D. Williams, *Geol. Soc. Spec. Publ.*, *44*, 3–15.

Wortel, M. J. R., and W. Spakman (2000), Subduction and slab detachment in the Mediterranean-Carpathian region, *Science*, *290*, 1910–1917.

Ziegler, P. A., S. Cloetingh, and J. D. van Wees (1995), Dynamics of intra-plate compressional deformation: The Alpine foreland and other examples, *Tectonophysics*, *252*, 7–59.

Zoetemeijer, R., Č. Tomek, and S. Cloetingh (1999), Flexural expression of European continental lithosphere under the western outer Carpathians, *Tectonics*, *18*, 843–861.

G. Bertotti, S. Cloetingh, K. Leever, and L. Matenco, Netherlands Centre for Integrated Solid Earth Sciences, Faculty of Earth and Life Sciences, Vrije Universiteit, De Boelelaan 1085, NL-1081 HV Amsterdam, Netherlands. (liviu.matenco@falw.vu.nl)

C. Dinu, Faculty of Geology and Geophysics, University of Bucharest, 6 Traian Vuia str., sect. 1, RO-70139, Bucharest, Romania.

S. M. Schmid, Geologisch-Paläontologisches Institut, University of Basel, Bernoullistr. 32, CH-4056 Basel, Switzerland.

M. Tărăpoancă, Rompetrol SA, Exploration& Production, 222 Calea Victoriei, RO-010099 Bucharest, Romania.